Research on the endocrine disrupting potential of environmental contaminants and their developmental toxicity using zebrafish

2023

CHEN Xing

Doctoral Program of
Veterinary Science

Graduate School of
Animal and Veterinary Sciences and Agriculture

Obihiro University of
Agriculture and Veterinary Medicine

ゼブラフィッシュを用いた環境汚染物質の内分泌撹乱作用と発生毒性に関する研究

令和５年

(2023)

帯広畜産大学大学院畜産学研究科

獣医学専攻博士課程

チャン　シン

Contents

Abbreviation **1**

General Introduction **4**

Objectives and chapter structures **8**

Chapter I. Establishing efficient *in vivo* and *in silico* methods to assess the anti-androgenic potential of environmental contaminants **9**

1.1. Introduction 9
1.2. Materials and methods 10
1.2.1. Chemicals 10
1.2.2. Zebrafish maintenance and breeding 11
1.2.3. Chemical exposures 11
1.2.4. Gene expression measured by quantitative real-time PCR 12
1.2.5. In silico homology modeling and docking simulation 13
1.2.6. Morphological assessments 14
1.2.7. Statistical analysis 15
1.3. Results 16
1.3.1. Stage-dependent effect of TES on sult2st3 mRNA expression 16
1.3.2. Effects of FLU and four pesticides on the 1-nM TES-induced expression of sult2st3 16
1.3.3. Effects of anti-androgens on the potentiation of high-concentration of TES-induced sult2st3 expression 17
1.3.4. Homology modelling and docking simulation 17
1.3.5. Morphological effects of anti-androgenic chemicals 18
1.4. Discussion 19
1.5. Conclusion 24

Chapter II. Evaluating anti-androgenic and anti-estrogenic potentials of BPA and its analogs and their developmental toxicity using zebrafish **34**

2.1. Introduction 34
2.2. Materials and methods 36
2.2.1. Chemicals 36

2.2.2. Zebrafish maintenance and breeding 37
2.2.3. Chemical treatments 37
2.2.4. Gene expression measured by quantitative real-time PCR 38
2.2.5. In silico homology modelling and docking simulation 38
2.2.6 Morphological assessments 40
2.2.7 Statistical analysis 40
2.3. Results 40
2.3.1. Anti-androgenic potency of BPA and its analogs in vivo 41
2.3.2. Anti-androgenic binding potentials of BPA and its analogs in silico 41
2.3.3. Anti-estrogenic potentials of BPA and its analogs in vivo 42
2.3.4. Anti-estrogenic binding potentials of BPA and its analogs in silico 42
2.3.5. Cardiovascular toxicity induced by BPA and its analogs 44
2.3.6. ICI effects on BPA and its analogs induced cardiovascular toxicity 44
2.4. Discussion 44
2.5. Conclusion 48
General Discussion 70
General Conclusion 72
Abstract 73
要約 78
References 84
Acknowledgment 102

Abbreviation

	2,2′-BPF	2,2′-bisphenol F
	20-OHT	20-hydroxyecdysone
	2D	Two-demensional structure
	3D	Three-demensional structure
	4-OHT	4-hydroxytamoxifen
A	ANOVA	Analysis of variance
	AR	Androgen receptor
B	Bis-MP	4,4′-(1,3-dimethylbutylidene)diphenol
	BP C2	Bisphenol C2
	BPA	Bisphenol A
	BPAF	Bisphenol AF
	BPAP	Bisphenol AP
	BPB	Bisphenol B
	BPE	Bisphenol E
	BPF	Bisphenol F
	BPP	Bisphenol P
	BPS	Bisphenol S
	BPZ	Bisphenol Z
C	*CYP19A1b*	Cytochrome P450 19A1b
	CYP2K22	Cytochrome P450 2K22
D	DDE	*p*,*p*′-DDE

	DHT	5α-dihydrotestosterone
	DMSO	Dimethyl sulfoxide
E	E2	17β-estradiol
	EC_{50}	50% effective concentration
	EDC	Endocrine disrupting chemical
	eef1a1l1	Elongation factor 1α1, like 1
	Emax	Maximum fold change relative to the vehicle control
	ERs	Estrogen receptors
F	FEN	Fenitrothion
	FLU	Flutamide
H	hAR	Human AR
	hERs	Human ERs
	hpf	h postfertilization
I	IC_{50}	50% inhibitory concentration
L	LBD	Ligand binding domain
	LBP	Ligand binding pocket
	LIN	Linuron
	LOEC	Lowest observed effect concentration
	Log Kow	Logarithmic n-octanol/water partition coefficient
M	MOE	Molecular Operating Environment Program
P	PP	Potassium permanganate
	PXR	Pregnane X-receptor
Q	qPCR	Quantitative real-time PCR
R	RR-THC	(R,R)-cis-Diethyl tetrahydro-2,8-chrysenediol

S	SEM	Standard error of the mean
	sult2st3	Sultfotransferase 2st3
T	TES	17α-methyltestosterone
V	VIN	Vinclozolin
Z	zfAR	Zebrafish AR
	zfERs	Zebrafish ERs

General Introduction

A significant and varied array of endocrine-disrupting chemicals (EDCs) has been released into the environment since World War II (Colborn et al., 1993). EDCs have the capacity to interfere with the normal functioning of the endocrine and reproductive systems by imitating or impeding the actions of endogenous hormones (Koninckx, 1999; Paulozzi, 1999; Swan et al., 2000; Waters et al., 2001).

For numerous years, researchers have recognized the potential harm posed by EDCs to aquatic species (Gilbertson et al., 1991). Notably, exposure to anti-androgens and estrogens has been linked to the feminization of wild fish (Gibson et al., 2005; Hill et al., 2010; Jobling et al., 2009). Given that anti-androgenic effects have been associated with reproductive toxicity (Hill et al., 2010; Martinović et al., 2008) and disruption of the endocrine system in fish (Ankley et al., 2005), it is crucial to identify environmental chemicals with anti-androgenic potential and to develop sensitive detection methods to assess anti-androgenic responses in fish.

Researchers have employed *in vitro* reporter gene assay systems, where Chinese hamster ovary cells or other cells are transfected with human nuclear receptors, to demonstrate the anti-androgenic, estrogenic, and anti-estrogenic potencies of various environmental chemicals (Araki et al., 2005; Kojima et al., 2004; Orton et al., 2011; Roy et al., 2004; Vinggaard et al., 2008). However, the translation of experimental findings concerning the human androgen receptor (AR) to the fish AR is a subject of debate due to potential species-specific variations in sensitivity to anti-androgens.

Several techniques have been developed to identify anti-androgenic effects in fish. The utilization of female three-spined stickleback (*Gasterosteus aculeatus*) as a model enables the measurement of Spiggin protein production, serving as an indicator for detecting anti-androgens (Jolly et al., 2009). Additionally, the papillary processes of juvenile Japanese medaka have been

employed as indicators to detect anti-androgenic activity (Nakamura et al., 2014). Furthermore, a *spiggin-gfp* medaka line has been created, incorporating the *spiggin* promoter from the three-spined stickleback and a fluorescent reporter gene, to facilitate the screening of (anti)androgens (Sébillot et al., 2014). It is important to note that these testing methods necessitate longer exposure durations (Jolly et al., 2009; Nakamura et al., 2014; Sébillot et al., 2014) and specific maintenance systems for the respective fish species (stickleback) and transgenic fish (*spiggin-gfp* medaka).

Zebrafish (*Danio rerio*) are cost-effective and efficient animal models as compared to other model organisms. Thus, zebrafish have been broadly used for drug screening, gene function analysing, developmental toxicity measuring, and endocrine-disrupting study. The single functional androgen receptor (AR) has been identified in zebrafish and androgens bind to it with a high affinity (Hossain et al., 2008; Jørgensen et al., 2007). Unlike mammals, zebrafish have three subtypes of estrogen receptors (ERs), namely ERα, ERβ1, and ERβ2 (Menuet et al., 2002), each playing shared and subtype-specific roles in regulating target genes, including cytochrome P450 19A1b (*CYP19A1b*) (Mouriec et al., 2009).

In recent years, molecular docking simulations have become an integral part of structure-based computational studies aiming to enhance our understanding of receptor-ligand interactions at the atomic level. Therefore, it is both possible and crucial to develop rapid and quantitative assessment methods for identifying anti-androgens *in vivo* and *in silico* using zebrafish. Additionally, this research applied the established anti-androgenic testing methods to exam various environmental contaminants, and measured their anti-estrogenic capabilities *in vivo* and *in silico*, as well as assessed their developmental toxicity. The brief diagram of this research project is shown in Fig. 1 and the chemical structures tested *in vivo* are shown in Fig. 2.

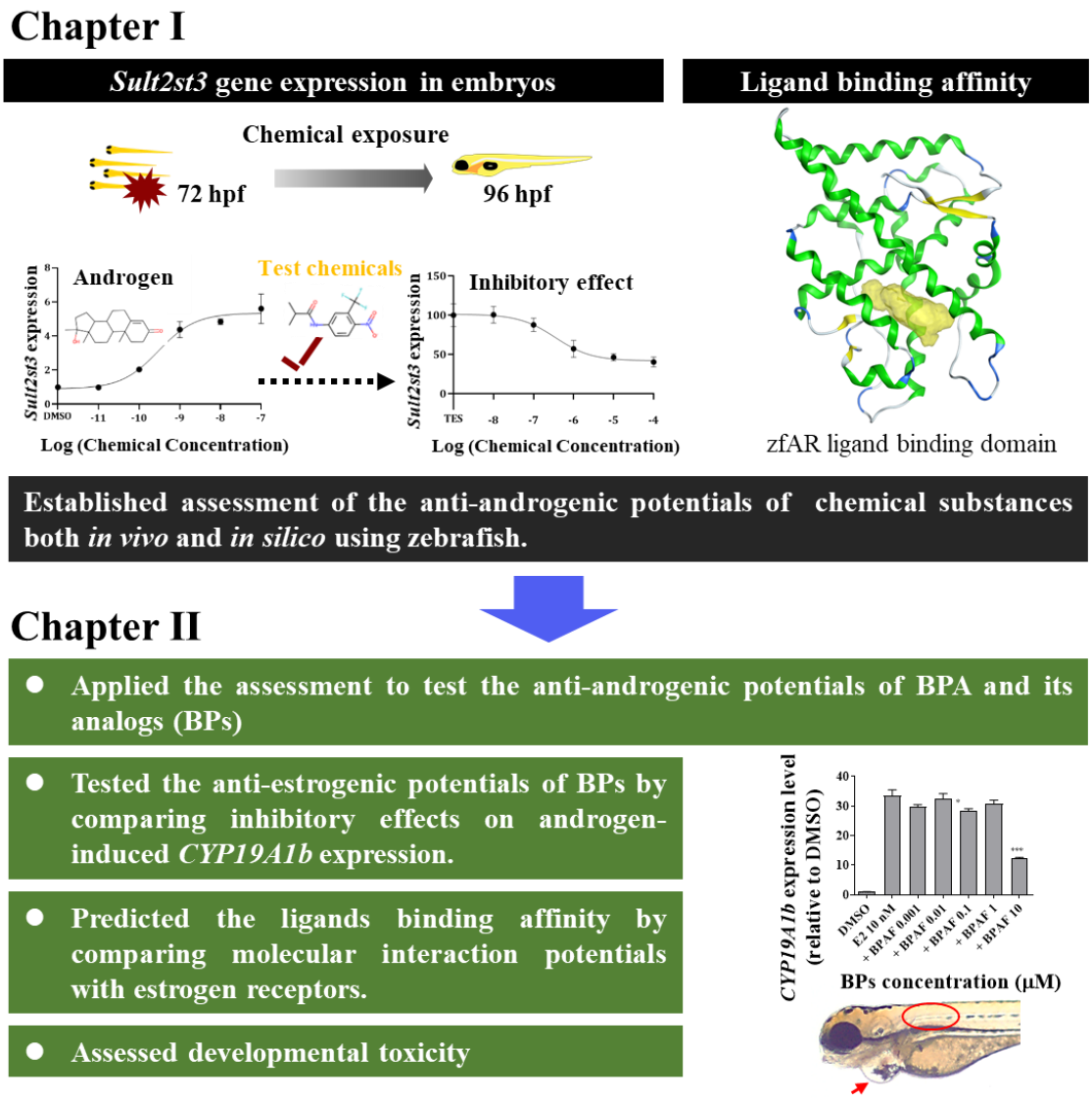

Fig. 1. Brief diagram of this project.

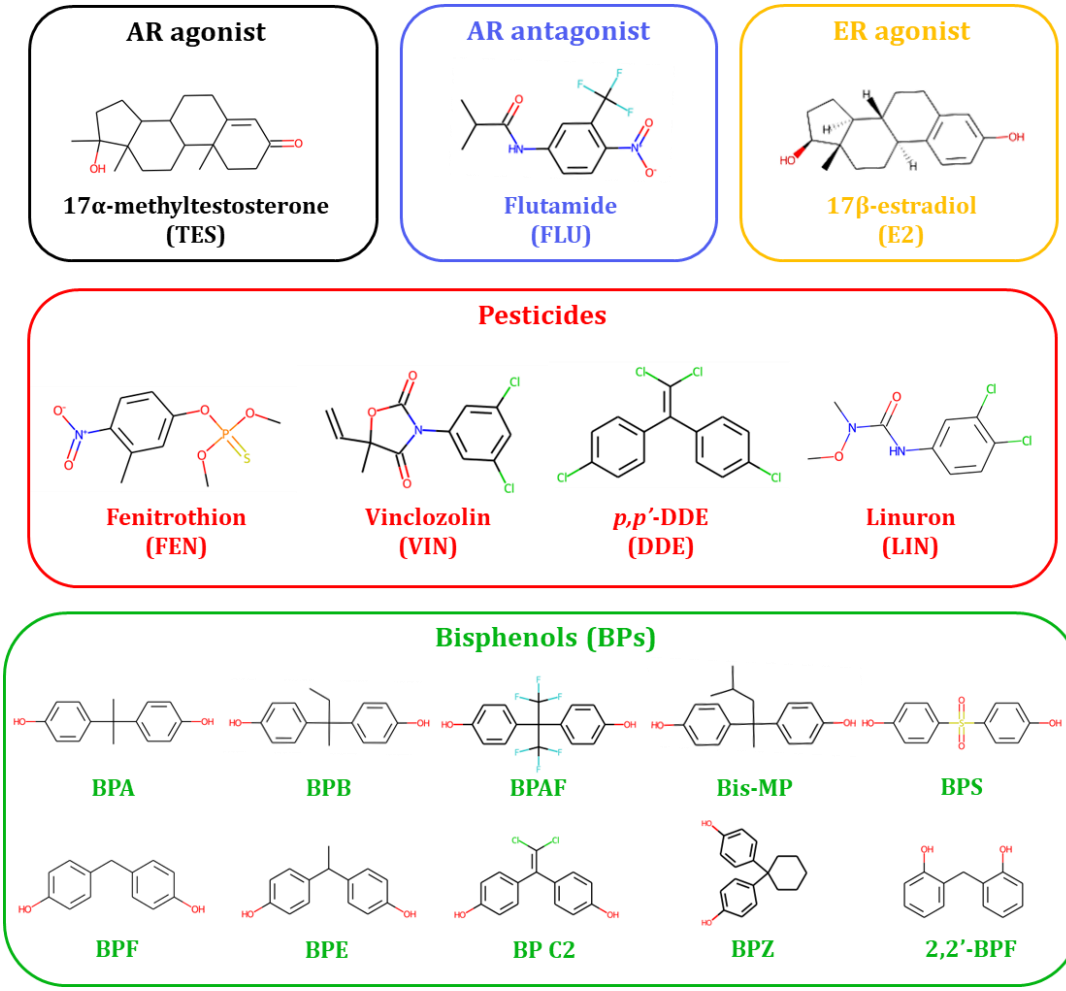

Fig. 2. Chemical structures tested *in vivo* in this research project. These structures were made from matplotlib and RDKit module in Python by Jae Seung Lee.

Objectives and chapter structures

The present study consists of 2 chapters:

Chapter I: This chapter aimed to establish zebrafish-based *in vivo* and *in silico* assay systems to evaluate the anti-androgenic potential of environmental chemicals. For *in vivo*, this chapter compared the inhibitory potency of test chemicals on androgen-induced sulfotransferase 2st3 (*sult2st3*) expression. For *in silico*, this chapter investigated the ligand binding affinities to zebrafish androgen receptor (zfAR). In order to explore the potential correlation between anti-androgenic potency and developmental toxicity, this chapter additionally examined various toxic endpoints commonly observed in developing zebrafish, including lethality, pericardial edema, blood flow reduction in trunk vessels, yolk-sac edema, and impaired swim bladder inflation.

Chapter II: This chapter applied the established method to evaluate the anti-androgenic potentials of BPA and its analogs in zebrafish *in vivo* and *in silico*. Also, this chapter measured the anti-estrogenic effects of BPA and its analogs by comparing the inhibitory effects on estrogen-induced cytochrome P450 19A1b (*CYP19A1b*) mRNA expression, as well as predicted the ligand binding affinity of these compounds to zebrafish estrogen receptor subtypes (zfERs) *in silico*. To better understand the involvement of ER signaling in developmental toxicity of BPA and its analogs, this chapter also conducted morphological assessments.

Chapter I. Establishing efficient *in vivo* and *in silico* methods to assess the anti-androgenic potential of environmental contaminants

1.1. Introduction

Zebrafish possess a single functional androgen receptor (AR) to which androgens exhibit strong binding affinity (Hossain et al., 2008; Jørgensen et al., 2007). The amino acid sequence of the zebrafish AR (zfAR) shares a high degree of identity with ARs from fathead minnow (Pimephales promelas; 84%) and goldfish (Carassius auratus; 84%), but displays relatively lower identity with the human AR (39%) (Hossain et al., 2008; Jørgensen et al., 2007).

The expression pattern of zfAR during development has been investigated. Hossain et al. (2008) observed that maternal zfAR transcripts are present in the embryos and persist until the 50% epiboly stage, but their levels significantly decline by the 5-somite stage (Hossain et al., 2008). Zygotic expression of zfAR can be detected as early as 24 h postfertilization (hpf), with expression levels increasing throughout development until the larval stage (at least 14 days postfertilization) (Hossain et al., 2008). In adult zebrafish, the AR is ubiquitously expressed in various tissues, including the gonads, brain, kidneys, liver, skin, muscles, and eyes (Hossain et al., 2008). Higher expression levels of AR are observed in the gonads and muscles of males compared to females (Hossain et al., 2008).

Previous research utilizing zebrafish embryos has demonstrated that the gene sulfotransferase family 2, cytosolic sulfotransferase 3 (*sult2st3*) and cytochrome P450 2K22 (*CYP2K22*) are responsive to androgens (Fent et al., 2018; Fetter et al., 2015; Willi et al., 2020). It has been observed that *sult2st3* exhibits a more stable response (lower within-group variation) compared to *CYP2K22* (Fetter et al., 2015). Based on these findings, we hypothesized that the anti-androgenic properties

could be assessed specifically by evaluating the androgen-induced expression level of *sult2st3* and its inhibition through exposure to test substances. Studies evaluating the concentration–anti-androgenic response relationships of various environmental chemicals are limited, although the anti-androgenic responses to nilutamide (a model anti-androgen) and vinclozolin (VIN; a common dicarboximide fungicide) have been investigated in zebrafish (Fetter et al., 2015; Jarque et al., 2019).

The objective of this chapter was to develop a rapid and efficient quantitative *in vivo* assay system for the identification of anti-androgens in fish. We achieved this by comparing the concentration-dependent inhibitory effects of chemicals on the androgen-induced expression of *sult2st3* in developing zebrafish. Specifically, flutamide (FLU), *p,p′*-DDE (DDE), VIN, linuron (LIN), and fenitrothion (FEN) were used as model compounds due to their known anti-androgenic activities in various assay systems, including *in vitro* and *in vivo* (Araki et al., 2005; Kelce et al., 1994; Kojima et al., 2004; McIntyre et al., 2001; Orton et al., 2011; Roy et al., 2004; Sebire et al., 2009; Vinggaard et al., 2008; Xu et al., 2006). In this chapter, the anti-androgenic potentials of these model compounds were also assessed using an *in silico* docking simulation of ligand binding with the zfAR. Furthermore, to investigate the potential correlation between anti-androgenic potency and developmental toxicity, we examined lethality and other toxic endpoints commonly observed in developing zebrafish, including pericardial edema, blood flow reduction in trunk vessels, yolk-sac edema, and impaired swim bladder inflation.

1.2. Materials and methods

1.2.1. Chemicals

Dimethyl sulfoxide (DMSO), DDE (CAS#72-55-9), VIN (CAS#50471-44-8), and FEN (CAS#122-14-5) were purchased from Wako Pure Chemical Industries (Osaka, Japan), whereas 17α-

methyltestosterone (TES; CAS#58-18-4), FLU (CAS#13311-84-7), and LIN (CAS#330-55-2) were purchased from Sigma-Aldrich (St. Louis, MO, USA). Stock solutions of each compound were prepared in DMSO, with a concentration 1000-fold higher than the exposure concentration, and stored at −30°C. These stock solutions were used within a two-month period.

1.2.2. Zebrafish maintenance and breeding

Male and female zebrafish (Danio rerio, wild-type AB strain), which were maintained in a zebrafish system (REI-SEA, Iwaki, Tokyo), were paired in a ratio of 4:3 for mating. The water quality was maintained to the standards previously described by Kubota et al. (2019). Eggs were collected and placed in polystyrene Petri dishes (15 cm in diameter) containing E3 medium (5 mM NaCl, 0.17 mM KCl, 0.33 mM $CaCl_2$, 0.33 mM $MgSO_4$, and 10^{-5}% methylene blue), and embryos were reared for 24, 48, 72, or 96 h in an incubator at 28.5°C under a 14/10-h light/dark cycle. Every 24 h, deformed or dead embryos were removed and water was refreshed. All experimental procedures were approved by the Animal Care and Use Committee of the Obihiro University of Agriculture and Veterinary Medicine (notification nos.: 19–32, 20–23, and 21–33).

1.2.3. Chemical exposures

To analyse gene expression, we conducted a single exposure study to investigate the concentration–response relationships of *sult2st3* mRNA expression in zebrafish at different developmental stages. Embryos at 24, 48, 72, and 96 hpf were exposed to either vehicle (0.1% DMSO, v/v) alone or various concentrations of TES (0.01, 0.1, 1, 10, and 100 nM) for 24 h. Subsequently, we conducted a coexposure study to assess the concentration-dependent effects of the test chemicals on TES-induced *sult2st3* expression. Embryos at 72 hpf were exposed to 0.1% DMSO (vehicle

control) or fixed concentration of TES (1 nM) in the presence or absence of different concentrations of FLU (0.001, 0.01, 0.1, 1, or 10 μM) or pesticides (DDE and VIN: 0.01, 0.1, 1, 10, or 100 μM; LIN: 0.1, 1, 10, or 100 μM; and FEN: 0.1, 1, 10, or 100 μM). We also assessed the effects of high concentrations of FLU or pesticides on TES-induced *sult2st3* expression. Specifically, embryos were coexposed to a fixed concentration of FLU (10 μM) or pesticides (DDE: 100 μM; VIN: 10 μM; and LIN: 100 μM) and different concentrations of TES (10 or 100 nM). Exposure was performed by adding 8 μL of chemical solution to a polystyrene Petri dish (5.5 cm in diameter) in the opposite position of the embryos (n = 20) and tilting the Petri dish to add 8 mL of E3 medium to the solution before swirling gently to mix thoroughly. Each treatment group consisted of four replicates. The embryos were kept at 28.5°C until the exposure process was ended, after which they were rinsed three times with breeding water, collected into MagNA Lyser Green Beads (Roche, Basel, Switzerland), flash-frozen in liquid nitrogen, and stored at −80°C until further experiments were conducted.

For morphological assessments, 10 embryos per Petri dish were exposed to vehicle or different concentrations of each chemical. The concentrations used were as follows: FLU (1, 3, 10, or 30 μM), DDE and FEN (1, 3, 10, 30, 100, or 300 μM), VIN (1, 3, 10, 30, or 100 μM), and LIN (3, 10, 30, 100, or 300 μM). The exposure was conducted from 72 to 96 hpf of embryos in 4 cm Petri dishes containing 4 mL of E3 medium, following a similar procedure for the gene expression analysis mentioned earlier. Four separate experiments were performed for each chemical, and each replicate included 10 embryos (n = 40).

1.2.4. Gene expression measured by quantitative real-time PCR

The isolation of total RNA was carried out using QIAzol Lysis Reagent (Qiagen, Maryland, USA) and a FastPrep24 Instrument ver.4 (MP Biomedicals, Santa Ana, CA). The purified RNA was obtained by following the instructions provided with the NucleoSpin kit (Macherey-Nagel, Düren,

Germany). The concentration and quality of the RNA were assessed using a NanoDrop ND-1000 (NanoDrop Technologies, Wilmington, DE, USA). For cDNA synthesis, 1 μg total RNA was reverse-transcribed using a Transcriptor First Strand cDNA Synthesis Kit (Roche, Mannheim, Germany). Quantitative real-time PCR (qPCR) was performed on a LightCycler 96 instrument (Roche) using the FastStart Essential DNA Green Master (Roche), as instructed by the manufacturer. A total volume of 20 μL was used to prepare the qPCR mixture, which included 10 μL of 2× FastStart Essential DNA Green Master, 250 nM of each primer, and 1 μL of cDNA template. qPCR runs were performed in duplicate for each gene. The primers used for eukaryotic translation elongation factor 1α1, like 1 (*eef1a1l1*; forward, 5′-CAACCCCAAGGCTCTCAAATC-3′; reverse, 5′-AGCGACCAAGAGGAG GGTAGGT-3′) (Goldstone et al., 2010) and *sult2st3* (forward, 5′-GACCACATCAAAAGCTGG CGAAAC-3′; reverse, 5′-GTGCTGTTACTGACGACACGATCC-3′) (Fetter et al., 2015) were synthesized by Eurofins Genomics (Tokyo, Japan). The qPCR program commenced with an initial denaturation step at 95°C for 10 min; followed by 55 cycles of denaturation at 95°C for 10s, annealing at 60°C for 10 s, and primer extension at 72°C for 10 s; and followed by 1 cycle of 95°C for 10 s, 65°C for 1 min, and 97°C for 1 s. After qPCR amplification, a melting curve analysis was conducted by maintaining the temperature at 95°C for 10 s, gradually decreasing to 65°C for 60 s, and then heating to 97°C for 1 s. To compare the relative expression levels of target genes in response to chemical exposure, the comparative threshold cycle method ($2^{-\Delta\Delta Ct}$) proposed by Livak and Schmittgen (2001) was applied.

1.2.5. In silico homology modeling and docking simulation

In silico analyses were conducted using the Molecular Operating Environment (MOE) Program developed by the Chemical Computing Group in Montreal, Canada. The amino acid sequence of zfAR was obtained from GenBank (accession no.: NP_001076592.1). The ligand binding domain

(LBD) of zfAR was chosen as the target sequence. To construct a homology model of zfAR, the MOE homology program was utilized, employing the crystal structure of human AR bound with hydroxyflutamide (PDB code: 2AX6) from the Protein Data Bank (http://www.rcsb.org) as a reference. The Structure Preparation module in MOE was employed to adjust structural defects and atom clashes. The amino acid sequence of zfAR was aligned with the refined human AR, and using the "induced fit" option, 10,000 structures of zfAR were generated, allowing the ligand to fit into the template structure. The generated structures were then optimized using the AMBER10:EHT force field (Labute and Williams, 2015) with solvation effects embedded in MOE. The optimal model structure was obtained using the Born/volume integral model parameters (Labute, 2008), and hydrogen atoms were added to the model using Protonate 3D.

The structures of the tested chemicals were obtained from the PubChem database in the form of an SDF file containing their two-dimensional (2D) structures. To create a chemical library with three-dimensional (3D) structures, structural conversion from 2D to 3D and geometry optimization were performed using Rebuild3d with the MMFF94x force field (Halgren, 1996). The docking simulation was carried out using MOE-Dock, and the energy of the ligand–zfAR complex was refined using the AMBER10:EHT force field. Each docking simulation was scored based on the lowest S-score (kcal/mol). The docking simulation was also applied to other three compounds that are not classified to anti-androgens, including potassium permanganate (PP) as a possible negative control (OECD, 2009), an anti-estrogenic compound 4-hydroxytamoxifen (4-OHT) (Löser et al., 1985), and a classical insect steroid hormone 20-hydroxyecdysone (20-OHE) (Wang et al., 2010).

1.2.6. Morphological assessments

At 96 hpf, we performed morphological assessments using an SZX10 stereomicroscope manufactured by Olympus in Japan. To determine the severity of pericardial edema and reduction in

blood flow, we employed a scoring system ranging from 0 to 2 (0, no effect; 1, mild effect; and 2, severe effect), according to our previous study (Lee et al., 2020). Additionally, we used the scoring system to evaluate the severity of yolk-sac edema (0 for normal yolk-sac, 1 for mild yolk-sac edema, and 2 for severe yolk-sac edema), as well as the degree of impaired swim bladder inflation (0 for fully inflated swim bladder, 1 for slightly inflated swim bladder, and 2 for non-inflated swim bladder).

1.2.7. Statistical analysis

In the analysis of gene expression, data are presented as the mean ± standard error of the mean (SEM) derived from four independent biological replicates. To determine the TES concentration-response relationship, we utilized a four-parameter logistic model, enabling the calculation of the 50% effective concentration (EC_{50}) and the maximum fold change relative to the vehicle control (E_{max}). Similarly, the concentration-response data concerning the inhibitory effects of the target substances on the TES-induced expression of *sult2st3* were fitted into a four-parameter logistic curve to determine the 50% inhibitory concentration (IC_{50}). The differences between each group at $P < 0.05$ were determined using one-way analysis of variance (ANOVA) with a post-hoc Tukey–Kramer test, and the tests were conducted using GraphPad Prism 8.4.3 (San Diego, CA).

For morphological evaluations, we presented the data as the mean percentage of each score of the observed endpoint in four separate experiments. Given the high reproducibility of morphological effects induced by each chemical across four separate experiments, statistical analysis was conducted using n = 40 embryos obtained from the amalgamation of the four separate experiments. Statistically significant differences in the numbers of affected (scored as “1,” “2,” and “dead”) and unaffected (scored as “0”) embryos between the DMSO (control) and exposure groups were evaluated using Fisher’s exact test for pairwise comparisons, and R version 4.0.4 (R Core Team, 2013) and various R

packages [tidyverse (Wickham et al., 2019) and RVAideMemoire (Herve, 2022)] were used to conduct the tests. All graphical representations were produced using GraphPad Prism.

1.3. Results

1.3.1. Stage-dependent effect of TES on sult2st3 mRNA expression

Concentration–response relationships were examined to evaluate the effects of TES on *sult2st3* mRNA expression during various stages of zebrafish development after a 24 h of exposure. A concentration-dependent rise in *sult2st3* expression was observed at 96 and 120 hpf, while no such increase was observed at 48 or 72 hpf (Fig. 3). The EC_{50} values for *sult2st3* expression were 0.30 and 0.29 nM at 96 and 120 hpf, respectively. As growth progressed, the maximum level of induction, represented as E_{max}, exhibited a slight increase, with 5.3- and 5.9-fold increases at 96 and 120 hpf, respectively. The fold change values reached a plateau in embryos collected at 96 hpf, prompting us to use 72–96 hpf as the exposure window for further evaluation of the anti-androgenic and morphological effects induced by FLU, DDE, VIN, LIN, and FEN.

1.3.2. Effects of FLU and four pesticides on the 1-nM TES-induced expression of sult2st3

FLU inhibited the 1-nM TES-induced expression of *sult2st3* in a concentration-dependent manner (IC_{50}: 5.7 μM; maximum inhibition: 92%; Fig. 4A). Of the pesticides, DDE had a concentration-dependent inhibitory effect on the 1-nM TES-induced expression of *sult2st3* (IC_{50}: 0.35 μM; Fig. 4B). TES-induced expression of *sult2st3* remained intact with exposure to the highest concentration of DDE (100 μM), at which point the inhibitory effect reached a plateau; thus, the maximum inhibitory effect achieved by DDE was 60%. Similarly, VIN and LIN inhibited the 1-nM

TES-induced expression of *sult2st3* in a concentration-dependent manner (IC_{50} values: 3.9 and 52 μM, respectively; Fig. 4C, D). The inhibition of *sult2st3* induction by VIN almost reached the level of the vehicle control (i.e., 93% inhibition). FEN couldn't get IC_{50} value for the inhibitory effect on the TES-induced expression of *sult2st3* in four parameter logistic regression, but it caused ~73% inhibition of this expression at the highest concentration tested (100 μM; Fig. 4E). All IC_{50} values for anti-androgenic potentials are shown in Table 1.

1.3.3. Effects of anti-androgens on the potentiation of high-concentration of TES-induced sult2st3 expression

Compared with TES alone, FLU (10 μM) decreased the 10-nM TES-induced expression of *sult2st3* significantly, whereas a lack of inhibition of *sult2st3* expression was observed with TES exposure at 100 nM (Fig. 5A). In contrast, DDE (100 μM) potentiated the induction of *sult2st3* by TES (10 or 100 nM) significantly (Fig. 5B). VIN (10 μM) also slightly enhanced the inducibility of *sult2st3* mRNA expression relative to that produced by 100-nM TES alone (Fig. 5C). LIN (100 μM) slightly reduced 10-nM TES-induced *sult2st3* expression but significantly potentiated 100-nM TES-induced *sult2st3* expression (Fig. 5D).

1.3.4. Homology modelling and docking simulation

The homology model for the LBD of zfAR closely resembled the X-ray crystal structure of human AR, with the root-mean-square distance found to be as low as 0.69 Å. The cavity volume of the zfAR ligand binding pocket (LBP) was calculated using Alpha Site Finder of MOE as 355.88 $Å^3$. The interaction energies of the tested chemicals with the zfAR LBD in *in silico* docking simulations are shown in Table 2. The interaction energies were divided into two branches by setting the line as

−5.0 kcal/mol. TES, FLU and the four tested pesticides had interaction energies below this line, whereas the negative control PP, anti-estrogen 4-OHT, and insect steroid hormone 20-OHE had interaction energies above the line.

The pure AR agonist TES interacted with zfAR LBD and hydrogen bonded with amino acids Arg702 and Asn655 (Table 2). The docking poses of FLU and the tested pesticides in the zfAR LBD are shown in Fig. 6. In the zfAR LBD, the nitro group of FLU is involved in two hydrogen bonds with Arg702 and one hydrogen bond with a backbone carbonyl group of Leu654. DDE, LIN, and FEN form a hydrogen bond with Arg702, whereas VIN forms a hydrogen bond between the oxazolidinedione ring oxygen and Gly658 (Table 2).

The amino acid residues that ligands interaction with zfAR in the LBP are shown in Fig. 7. The residue numbers located within 4.5 Å against each ligand are 17 for FLU and LIN, 18 for DDE and FEN, and 19 for VIN. In this range (4.5 Å), FLU and the four tested pesticides are surrounded by similar types and nearly equal numbers of amino acid residues.

1.3.5. Morphological effects of anti-androgenic chemicals

The percent incidences of mortality, pericardial edema, yolk-sac edema, reduction in blood flow, and impaired swim bladder inflation caused by FLU, DDE, VIN, LIN, and FEN are shown in Fig. 8. The mortality of zebrafish embryos was significant in embryos exposed to 30 μM FLU, 300 μM LIN, and 100 μM FEN. LIN and FEN exposures at 100 μM caused significant increases in the percent incidences of pericardial edema, yolk-sac edema, and reduction in blood flow. Exposure to most of the tested chemicals resulted in impaired swim bladder inflation in a concentration-dependent manner among the surviving embryos. The lowest observed effect concentration (LOEC) values for developmental toxicity are shown in Table 1.

1.4. Discussion

The present study showed that the *sult2st3* gene expression is sensitive to the exposure of androgen TES in the late stages of zebrafish embryonic development (Fig. 3). However, the significant upregulation of *sult2st3* by TES was reduced not only by FLU but also by four tested pesticides known to have anti-androgenic activities, DDE, VIN, LIN, and FEN (Fig. 4). These findings suggest that *sult2st3* could serve as a biomarker for screening anti-androgenic compounds in zebrafish embryos.

Our results concerning the response of *sult2st3* expression to TES align with previous studies conducted on zebrafish embryos exposed to androgens, which reported induction of this gene at 96 or 120 hpf (Fent et al., 2018; Fetter et al., 2015; Jarque et al., 2019). Additionally, alterations in *sult2st3* expression at 120 hpf were observed in embryos exposed to 500 nM of 11-ketotestosterone for varying durations (1–96 h) (Fetter et al., 2015), wherein a significant increase and peak induction were observed at 8 and 96 h of exposure, respectively. These results indicate the influence of both the exposure window and duration on the impact of androgens on *sult2st3* expression.

In the present study, DDE exhibited an IC_{50} value 11- and 16-fold lower than VIN and FLU (Table 1), respectively, indicating that DDE possesses the highest anti-androgenic potency among the tested chemicals, surpassing even the positive control FLU. Conversely, an IC_{50} could not be determined for the anti-androgenic potency of FEN, largely due to lethality in embryos at 300 μM. Previous human AR reporter gene assays have demonstrated that FEN exhibits nearly equivalent potency to VIN and surpasses both DDE and LIN (Kojima et al., 2004; Orton et al., 2011; Vinggaard et al., 2008). Thus, the order of anti-androgenicity observed in zebrafish embryos for the tested chemicals (i.e., DDE > VIN > LIN > FEN) differs somewhat from the order reported in *in vitro* assays involving the human AR.

To comprehend the factors influencing the variations in the order of anti-androgenic potency among the tested chemicals in zebrafish embryos and the aforementioned studies, we first directed our attention toward the membrane permeability of the chemicals, as it could contribute to differences in their incorporation levels. The logarithmic n-octanol/water partition coefficient (log Kow) of organic compounds has been extensively documented due to its close association with the bioconcentration factor and toxicity (Amutova et al., 2021; Di Toro et al., 2007). Dishaw et al. (2014) demonstrated that the tissue concentration of organophosphate flame retardants increased in 1 dpf zebrafish embryos following a day of exposure at 1 μM, with a positive correlation to higher log Kow values (Dishaw et al., 2014). Another study revealed the anti-androgenicity of bisphenols had a positive correlation with the log Kow in the human AR reporter gene assay system in recombinant yeast (Conroy-Ben et al., 2018). According to data obtained from PubChem, the log Kow value of DDE (6.51) is significantly higher than those of VIN (3.10), FLU (3.35), LIN (3.20), and FEN (3.30). Correspondingly, DDE showed the strongest *in vivo* anti-androgenic potency in the present study, potentially reflecting (at least in part) its efficient incorporation into the embryos. However, considering the similarly log Kow values of FEN, FLU, LIN, and VIN, differences in their lipophilicity may not account for the differences in their IC_{50} values.

Species-specific differences in the AR might also contribute to the different orders of anti-androgenicity. Various studies have been reported that dihydrotestosterone, ketotestosterone, testosterone, and androstenedione exhibit varying binding affinities to the AR in different species, including zebrafish, three-spined sticklebacks, and humans (Hossain et al., 2008; Ikeuchi et al., 2001; Jørgensen et al., 2007; Olsson et al., 2005). For instance, several human anti-androgens fail to inhibit 11-ketotestosterone-induced activation of stickleback AR (Lange et al., 2015). Furthermore, FEN shows much weaker anti-androgenic potency than FLU, VIN, and LIN in zebrafish and *spiggin-gfp*

medaka (Sébillot et al., 2014), while exhibiting the strongest anti-androgenic activity among these chemicals in three-spined sticklebacks (Jolly et al., 2009).

DDE only achieved a 60% inhibitory effect on TES-induced *sult2st3* expression even at the highest tested concentration (100 μM), which could be attributed to its specific features. Previous studies have indicated that DDE exhibits agonistic features with respect to the estrogen receptor (ER), pregnane X-receptor (PXR), and constitutive androstane receptor, while displaying antagonistic features towards the AR, progesterone receptor, and glucocorticoid receptor (Kretschmer and Baldwin, 2005; Li et al., 2008; Yang et al., 2010; Zhang et al., 2016). PXR has also been implicated in the regulation of sulfotransferase transcript expression in human hepatocytes and mice (Alnouti and Klaassen, 2008; Duanmu et al., 2002). In the present study, rather than suppressing the induction of *sult2st3* caused by exposure to low-concentration of TES, DDE enhanced *sult2st3* expression compared to that induced by exposure to a high-concentration of TES (Fig. 5), suggesting that DDE activated other nuclear receptors to enhance high-concentration TES-induced *sult2st3* expression.

LIN has been characterized as an anti-androgen both *in vitro* studies involving human, rat, and three-spined stickleback (Jolly et al., 2009; Lambright et al., 2000) and *in vivo* studies involving rat, three-spined stickleback, and Japanese medaka (Jolly et al., 2009; Lambright et al., 2000; Sébillot et al., 2014). In the present study, LIN exhibited a weak anti-androgenic potency towards the zfAR, consistent with findings reported for the human and rat ARs (Freyberger et al., 2010; Serçinoğlu et al., 2021). Furthermore, aside from its anti-androgenic potency, LIN has demonstrated anti-estrogenic activity in medaka (Spirhanzlova et al., 2017) and estrogenic activity in zebrafish embryos (Quintaneiro et al., 2017). A previous study revealed that 17β-estradiol upregulated *sult2st3* mRNA expression during the late developmental stage of zebrafish embryos (Schmid et al., 2020). Hence, it is plausible that the ER may mediate the effects of LIN on high-concentration TES-induced expression of *sult2st3* (Fig. 5).

We observed a consistent impact on the degree of swim bladder inflation resulting from exposure to FLU, DDE, VIN, LIN, and FEN exposure (Fig. 8). The LOECs for impaired swim bladder inflation were as follows: FLU (10 μM), VIN/FEN (30 μM), LIN (100 μM), and DDE (300 μM) (Table 1). Despite DDE exhibiting the highest anti-androgenic potency, it only showed significant effect on the occurrence of impaired swim bladder inflation at the highest tested concentration (300 μM). FEN, however, displayed equivalent effects on swim bladder inflation to VIN, despite its relatively low anti-androgenic potency. This suggests that anti-androgenic potency does not determine the occurrence of anti-androgen-induced impaired swim bladder inflation. During our assessment of other endpoints, we observed mortality in embryos exposed to high concentrations of FLU, LIN, and FEN, but not DDE or VIN (Fig. 8). Furthermore, both LIN and FEN caused various developmental toxicities, including pericardial edema, yolk-sac edema, and blood flow reduction (Fig. 8). Hence, it is unlikely that the developmental toxicities induced by these anti-androgens have a clear relationship with their anti-androgenic potency, as measured by their effects on *sult2st3* expression levels.

All of the chemicals examined in the present study have been detected in the aquatic environment. DDE was found in water samples collected from 10 points of the River Benue, Yola, Adamawa State, Nigeria in 2015, at concentrations as high as 590 μg/L (1.9 μM), possibly due to the continued use of DDT in the area after its ban in 2008 (Akan et al., 2015). A 2022 study also reported DDE contamination at 0.31 μg/L (0.00097 μM) in Gibe River water (Jemal et al., 2022). In the southern Dead Sea basin, VIN was detected in groundwater at concentration ranging from 60–220 μg/L (0.21–0.77 μM) and in surface water at concentration ranging from 128–390 μg/L (0.45–1.4 μM) (El-Shahat et al., 2003). The maximum concentration of VIN in the Bia and Tanoe Rivers of West Africa was reported as 9 μg/L (0.031 μM) (Siriki et al., 2021). In the same region, LIN was detected at a concentration of 0.3 μg/L (0.0012 μM) (Siriki et al., 2021). Several decades ago, LIN was detected in Canada surface water and groundwater at much higher levels of 1100 μg/L (4.4 μM) and 2800

μg/L (11 μM), respectively (Caux et al., 1998). FEN has been detected in river water samples from Tokyo and stream water samples from Kanagawa at levels as low as 0.083 μg/L (0.00030 μM) and 0.16 μg/L (0.00058 μM), respectively (Kameya et al., 2012). However, the range of FEN concentrations in water samples collected from lakes adjacent to agricultural fields in Savar, Bangladesh, was reported as 5.83–33.41 μg/L (0.021–0.120 μM) (Hossain et al., 2015). Although the environmental levels reported in the literature are generally lower than the IC_{50} values associated with anti-androgenic effects observed in zebrafish after short-term exposures, it is challenging to conclude that the contamination of DDE, VIN, LIN, and FEN in aquatic environments poses no threat to aquatic animals in terms of endocrine disruption and reproductive impairment. Notably, in some African countries where DDT is still used as an indoor residual spray to prevent malaria, the concentration of DDE in the river waters might exceed the threshold for inducing anti-androgenic effects in fish.

To assess the binding mode and potency of anti-androgenic compounds to the zfAR, we constructed an *in silico* homology model of the zfAR LBD and conducted a docking simulation (Table 2, Fig. 6 and 7). The volume of the potential LBP in the zfAR LBD model (355.88 $Å^3$) closely resembled the accessible pocket volume of human AR (341 $Å^3$) reported by Poujol et al. (2000), suggesting conservation in the three-dimensional shapes of the zfAR LBP and human AR LBP. Our docking simulation revealed that the binding potencies of the anti-androgenic pesticides to the zfAR were strongly correlated with the number of hydrogen bonds formed with key amino acid residues in the zfAR and the specific types of amino acid residues involved in these bonds. FLU formed three hydrogen bonds through interactions with Arg702 and Leu654 of the zfAR LBD resulting the lowest interaction energy. DDE, LIN, and FEN formed hydrogen bonds with Arg702, whereas DDE and LIN formed hydrogen bonds with Arg702 through halogen (Aullón et al., 1998), potentially explaining their relatively weak binding potencies with the zfAR. In fact, Asn705, Gln711, Arg752 (corresponding to Arg702 in zfAR), and Thr877 in the human AR have been reported to form

favorable hydrogen bonds with ligands (reviewed by Tan et al., 2015). Indeed, the endogenous ligand TES formed two hydrogen bonds with Asn655 and Arg702 in the zfAR LBD, exhibiting slightly higher interaction energy than the tested anti-androgenic ligands, suggesting that agonists or endogenous ligands may require specific binding to Asn655. Additionally, the Gly residue at position 708 in the human AR, corresponding to Gly658 in zfAR, plays a role in specific recognition of androgen ligands (Terouanne et al., 2003). Hence, the polar and hydrophobic interactions mediated by these amino acid residues in the zfAR are crucial for binding and anti-androgenic activity.

In general, FLU, DDE, VIN, LIN, and FEN, which demonstrated anti-androgenic potential *in vivo*, exhibited relatively lower interaction energies compared to the negative control PP, anti-estrogen 4-OHT, and insect steroid hormone 20-OHE (Table 2). A consensus interaction mode, with at least a hydrogen bond being formed with Arg702, was observed in the zfAR LBD. Docking simulations based on their interaction energies indicated that LIN and FEN displayed weaker binding potencies to zfAR compared to FLU, which aligns well with our *in vivo* findings. DDE and LIN exhibited higher interaction energies than FEN and VIN in the docking simulations (Table 2), which is consistent with the results of an *in vitro* study conducted on human AR-transformed MDA-kb2 cells, where FEN and VIN exhibited more potent anti-androgenic effects than DDE, and LIN showed the weakest anti-androgenic potency among the tested chemicals (Orton et al., 2011). The predicted rank order of ligand–AR binding potency from *in silico* analysis somewhat differs from the *sult2st3* induction potency estimated in zebrafish embryos. However, the *in silico* binding potency primarily relies on the ligand interaction with key amino acid residues, whereas the *in vivo* response can be influenced not only by the AR but also by other pathways, potentially including PXR and the ER (as mentioned above).

1.5. Conclusion

We discovered that *sult2st3* serve as an effective biomarker for both identifying environmental anti-androgens and assessing their anti-androgenic potency. This study provides novel zebrafish-based *in vivo* and *in silico* methods that enable rapidly and straightforward evaluation of the anti-androgenic potencies of various environmental chemicals. However, caution is necessary when relying solely on *sult2st3* expression as a measure for evaluating anti-androgenic potencies since this gene is regulated by multiple nuclear receptor signaling pathways. Notably, *in vivo* assessments of anti-androgenic potency based on nominal concentrations may underestimate the inherent potencies of more hydrophilic compounds. Additionally, this study established a potential computing method for screening anti-androgenic pollutants in zebrafish and identified that Arg702 plays pivotal role in the binding of anti-androgenic pesticides with the zfAR LBP. Therefore, employing *in silico* analysis to identify the binding characteristics of ligands with the zfAR can provide insights into the anti-androgenic potentials of untested compounds in zebrafish embryos.

Table 1. The IC_{50} values for the anti-androgenic potency and LOECs for the developmental toxicity of each chemical tested.

Compound	IC_{50} (μM)	LOEC (μM)				
		Pericardial edema	Yolk-sac edema	Blood flow reduction	Swim bladder inflation	Lethality
FLU	5.7	NA	NA	NA	10	30
DDE	0.35	NA	NA	NA	300	NA
VIN	3.9	NA	NA	NA	30	NA
LIN	52	100	100	100	30	300
FEN	NA	100	100	100	30	100

NA: no data available

Table 2. Interaction energies and key amino acid residues of ligands binding with the zfAR LBD.

Compound	S-score (kcal/mol)	Hydrogen bonding
TES	-5.9	Arg702, Asn655
FLU	-7.41	Arg702, Leu654
DDE	-6.38	Arg702
VIN	-6.86	Gly658
LIN	-6.33	Arg702
FEN	-7.19	Arg702
PP	-3.31	—
4-OHT	-4.44	—
20-OHE	-1.77	—

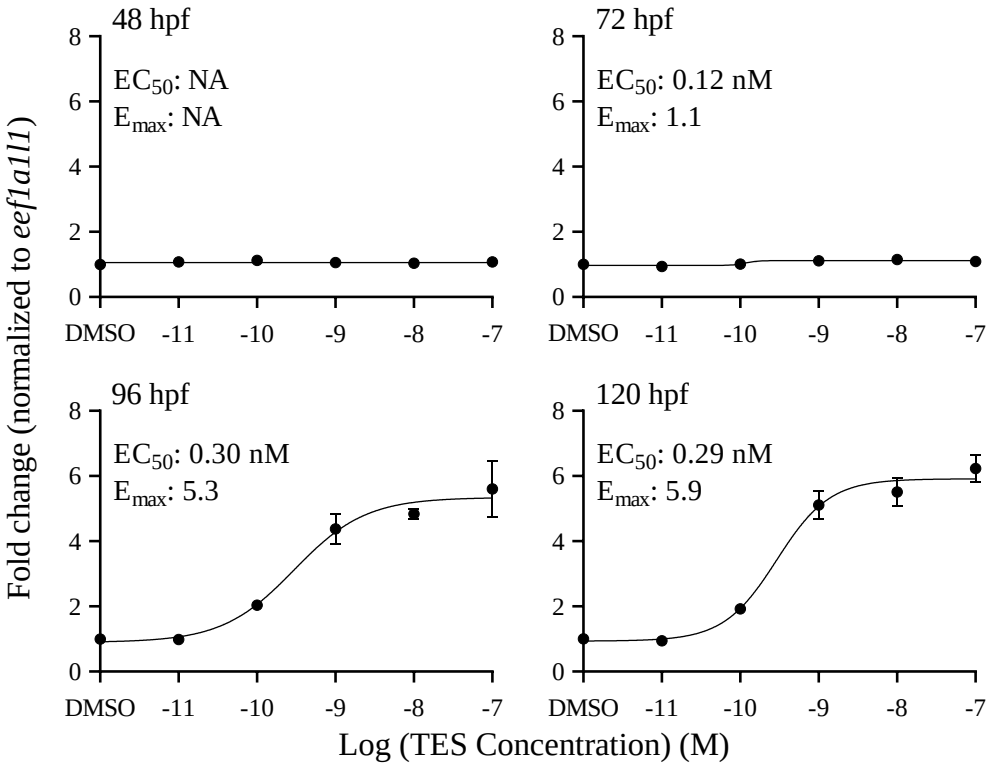

Fig. 3. Concentration–response relationships for the effects of TES on *sult2st3* mRNA expression in zebrafish at the different developmental stages. Data points represent mean fold change values relative to the DMSO control (n = 4) with the SEM.

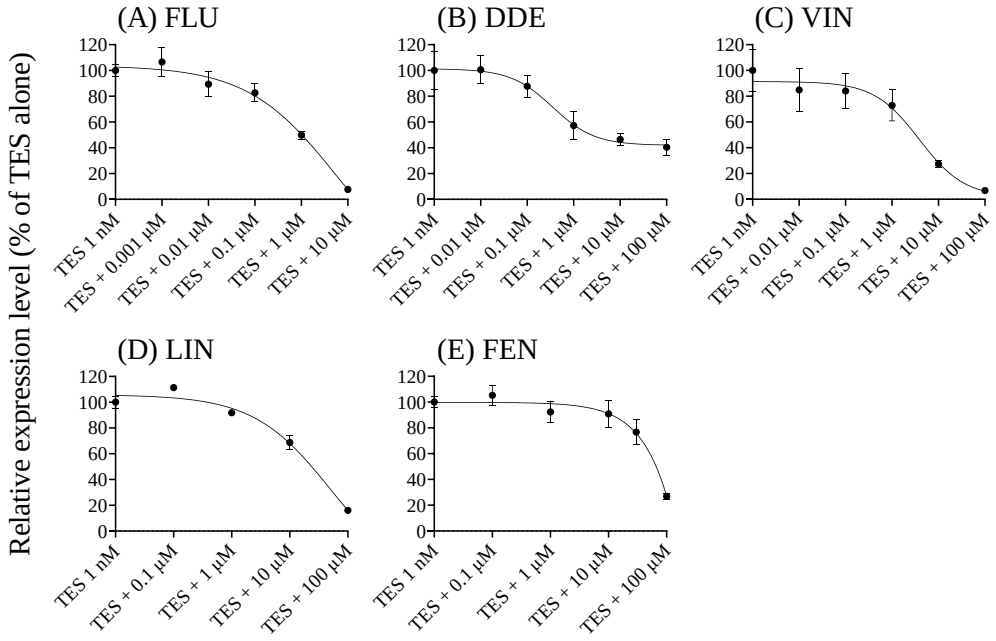

Fig. 4. Effects of anti-androgens on 1-nM TES-induced *sult2st3* mRNA expression at 96 hpf in zebrafish. Data represent mean percentages of 1-nM TES-induced expression of *sult2st3* (n = 4) with SEM.

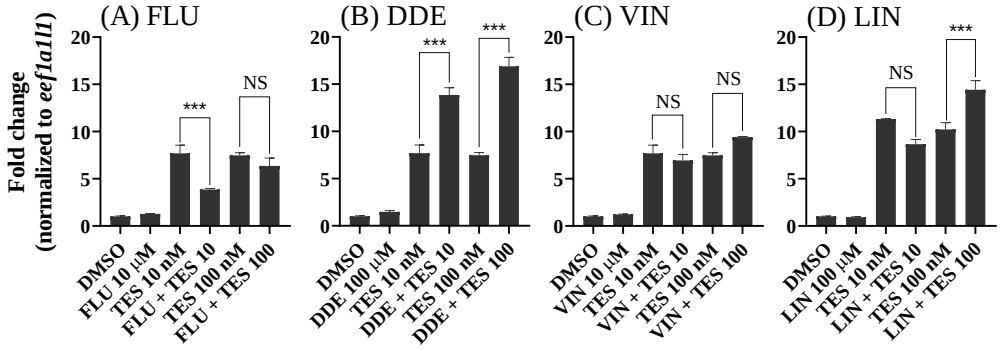

Fig. 5. Effects of anti-androgens on the potentiation of *sult2st3* expression induced by higher concentration of TES in zebrafish embryos at 96 hpf. Data represent mean fold change values relative to the DMSO control (n = 4) with the SEM. NS denotes no significant difference. *** $P < 0.001$.

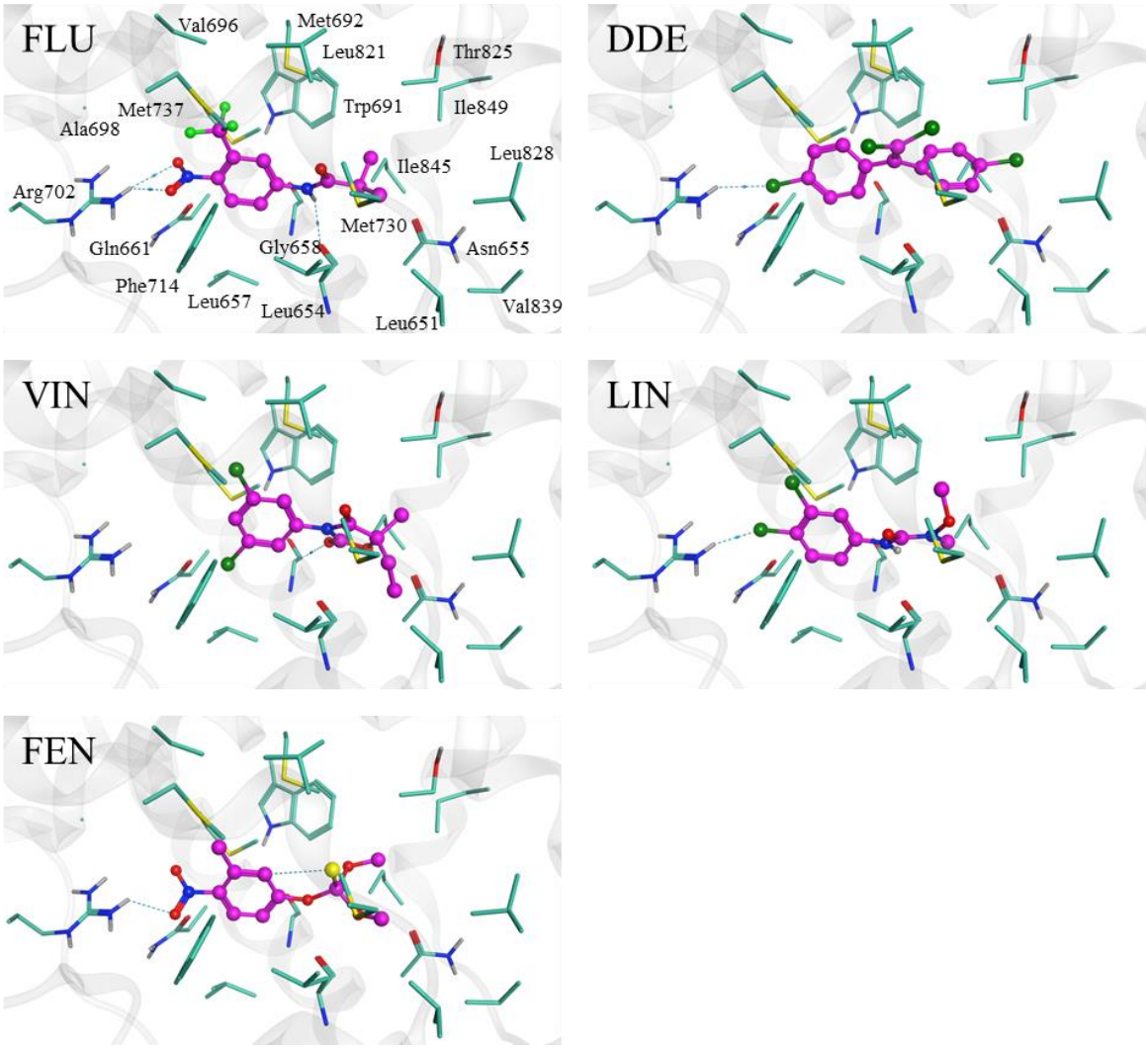

Fig. 6. Docking poses of FLU and the tested pesticides to the zfAR. The green dotted lines indicate the hydrogen bonds of the interaction between the hydroxyl group of each ligand and key amino acid residues.

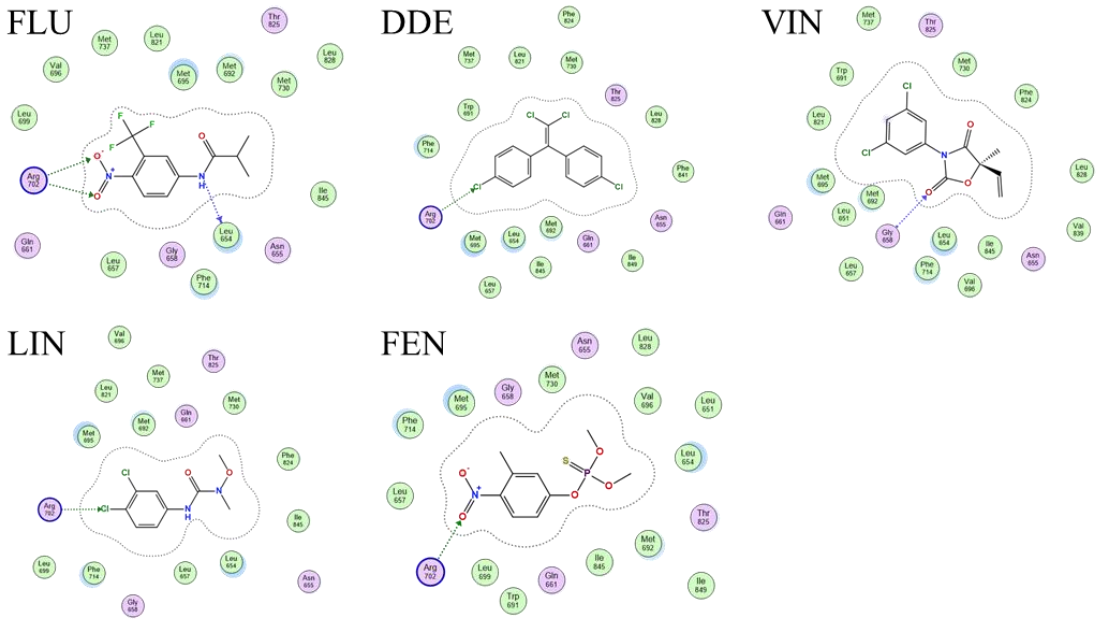

Fig. 7. Binding modes of FLU and pesticides in zfAR LBP. The dashed lines with arrow indicate a hydrogen bond formed by FLU (A), DDE (B), VIN (C), LIN (D) or FEN (E) with polar residues (colored in light purple) or hydrophobic residues (colored in light green).

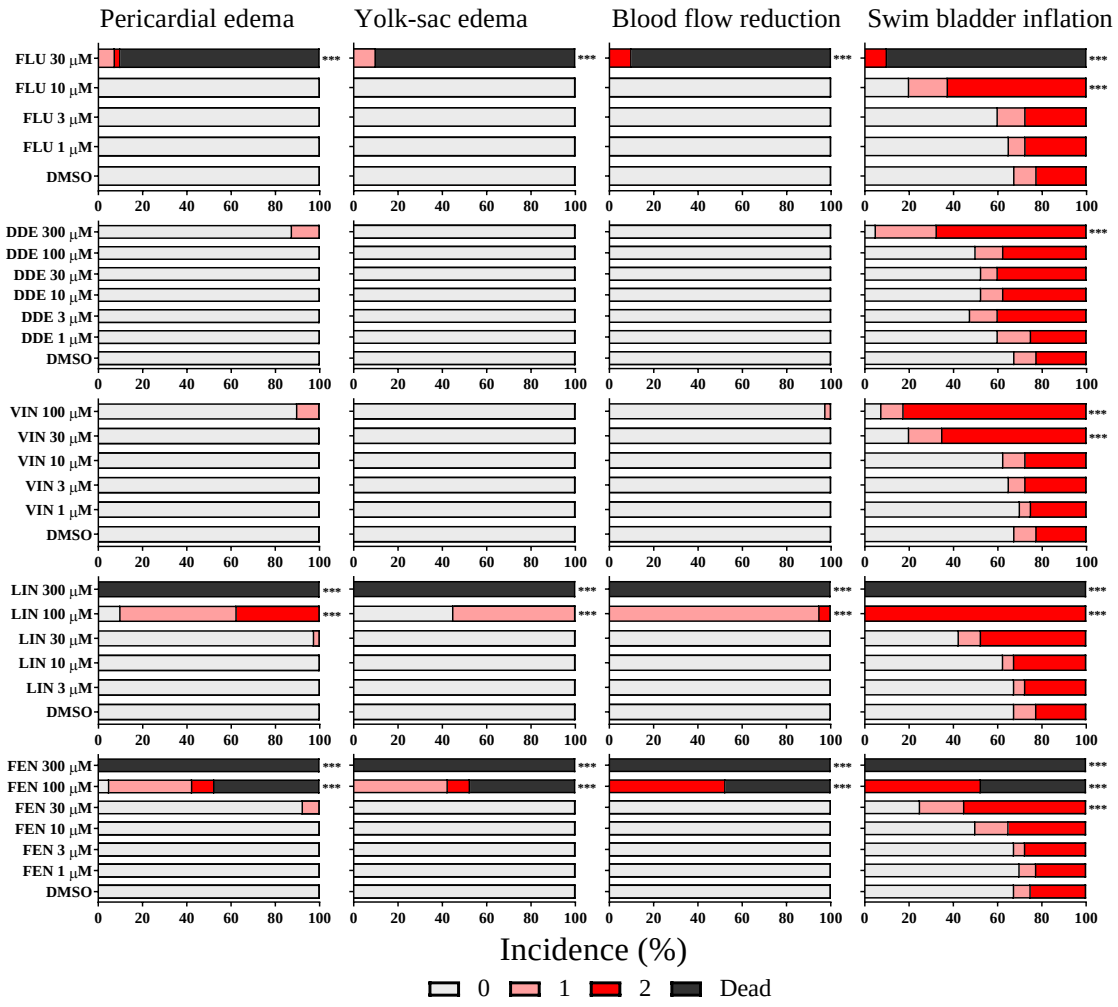

Fig. 8. Incidence of pericardial edema, yolk-sac edema, blood flow reduction and delayed inflation of swim bladder. The severity of each endpoint was scored between 0 and 2, (0, no effect; 1, mild effect; and 2, severe effect). Affected embryos were represented as percentages of total number of embryos at the beginning of exposure based on four separate experiments. Statistically significant differences in the numbers of affected (scored as "1," "2," and "dead") and unaffected (scored as "0") embryos between the DMSO and exposure groups were evaluated using Fisher's exact test for pairwise comparisons (* $P < 0.05$, *** $P < 0.001$, n = 40).

Chapter II. Evaluating anti-androgenic and anti-estrogenic potentials of BPA and its analogs and their developmental toxicity using zebrafish

2.1. Introduction

Bisphenol A (BPA) has been identified as an endocrine disruptor. It has been largely used in manufacture productions, including polycarbonate plastics, epoxy resins, and thermal paper (EFSA, 2015). The exposure to BPA is extensive via food, consumer products, and environmental sources (EFSA, 2015). As it was reported that BPA broadly detected (>97%) from the gestational (median: 2.0 μg/L) and childhood urine samples (median: 4.1 μg/L) collected from 244 mothers and their 3-year-old children from the greater Cincinnati, Ohio (Braun et al., 2011). It also has been detected from canned food and biological fluid (Braun et al., 2011; Cao et al., 2015; Deceuninck et al., 2015; Ikezuki et al., 2002).

Outcomes of BPA have been widely reported in vertebrates. Prenatal exposure to BPA affected offspring in aspect of mammary gland development (Muñoz-de-Toro et al., 2005), brain development (Wang et al., 2014), reproductive function (Wei et al., 2020), and behavior in rodents (Harris et al., 2018; Kundakovic et al., 2013; Xu et al., 2010). BPA disrupted spermatogenesis through apoptosis of germ cells and Leydig cell in goldfish, and the disruption cannot be recovered after BPA treatment withdrawals (Wang et al., 2019). Similarly, in human, exposure to BPA has been associated to reproductive and developmental effects, metabolic disease and others (Rochester, 2013).

The increasing concern over BPA leads to the increasing use of its analogs, as well-known bisphenol S (BPS) and bisphenol F (BPF). BPS and BPF have the similar potency (estrogenic, anti-estrogenic, androgenic and anti-androgenic) in the same order of magnitude as BPA (Rochester and

Bolden, 2015). Other influences such as oxidative stress, immune responses, teratogenic effects, steroidogenic alterations, and reproductive toxicity of BPF and BPS toward aquatic organisms have been further identified in recent studies (Moreman et al., 2017; Park et al., 2018; Qiu et al., 2018). However, as the major substitute, BPF appears in a variety of environmental medium, such as indoor dust, sediment, and water (Liao et al., 2012c, 2012b; Yan et al., 2017). BPF has been detected from surface water samples at the range of 0.0068–2.8 μg/L (0.034-13.98 nM) (Jin and Zhu, 2016; Yan et al., 2017; Zhang et al., 2019). It also detected in sewage and sediments at concentrations ranging from 0.022 to 0.123 μg/L (0.11-0.61 nM) and 1.2 to 7.3 μg/kg, respectively (Fromme et al., 2002). BPF is a significant contaminant in waters in several Southeast Asian countries (Jie et al., 2018; Yamazaki et al., 2015). The concentration of BPF is 1-2 orders of magnitude higher than that of BPA in water samples collected from river and sea of Japan, South Korea, and China, reaching 2850 ng/L (12.5 nM) in the Tamagawa River in Japan (Yamazaki et al., 2015). BPS was detected in 81% of 315 human urine samples from different countries, including Japan, China, United States, Kuwait, Vietnam, Malaysia, India, and Korea, at concentrations ranging from 0.02-21 μg/L (0.080-83.9 nM) (Liao et al., 2012a). Therefore, the studies on other analogs of BPA are required.

Research on BPA anti-androgenic activity has produced controversial data. A recent study showed BPA as an androgen receptor (AR) antagonist, preventing endogenous androgens from regulating androgen-dependent transcription and inhibiting Sertoli cell proliferation (Wang et al., 2017). An *in vitro* study showed that BPA is able to block the AR-mediated gene expression competing with 5α-dihydrotestosterone (DHT) to bind AR, revealing a significant inhibitory effect on the DHT-induced transcriptional activity (Sun et al., 2006). Contrary, another *in vitro* study showed that, following treatment with BPA, the inhibition of AR is partial and it lacks of a dose-response relationship, suggesting a non-competitive mechanism (Lee et al., 2003).

The endocrine disrupting effects of highly manufactured bisphenols (BPA, BPS, and BPF) are known, however the activities of most BPs are rarely understood. Zebrafish-based *in vivo* and *in silico* assessment methods have been established to exam the anti-androgenic potency for environmental pollutants in the Chapter I and published in an international journal (Chen et al., 2023). The present chapter applied the established assays to determine the anti-androgenic potentials of BPA and its analogs at lower concentrations in early developmental zebrafish. As well, this chapter determined their anti-estrogenic potentials through measuring the estrogen responsive gene cytochrome P450 2K22 (*CYP191b*) mRNA expression level, and their ligand-binding affinity of BPs to zebrafish estrogen receptor subtypes (ERs) using *in silico* docking simulation. To better understand the involvement of estrogen receptor (ER) signaling in developmental toxicity of BPA and its analogs, this chapter also conducted morphological assessments of cardiovascular toxicity, such as pericardial edema and blood flow reduction.

2.2. Materials and methods

2.2.1. Chemicals

All chemicals were purchased from company, dimethyl sulfoxide (DMSO), 17α-methyltestosterone (TES; CAS#58-18-4), 17β-estradiol (E2; CAS#50-28-2), fulvestrant (ICI; CAS#129453-61-8), BPA (CAS#80-05-7), BPF (CAS#620-92-8), bisphenol AF (BPAF; CAS#1478-61-1), bisphenol C2 (BP C2; CAS#14868-03-2), bisphenol Z (BPZ; CAS#843-55-0), 2,2′-bisphenol F (2,2′-BPF; CAS#2467-02-9), bisphenol E (BPE; CAS#2081-08-5), bisphenol B (BPB; CAS#77-40-7), BPS (CAS#80-09-1), and 4,4′-(1,3-dimethylbutylidene)diphenol (Bis-MP; CAS#6807-17-6). The detailed information was listed in Table 3. Compounds were dissolved in DMSO and stock

solutions were prepared as 1000 folds of exposure concentration. All stock solutions were stored at −30°C and used out within two months.

2.2.2. Zebrafish maintenance and breeding

The zebrafish embryos were obtained through breeding of adult zebrafish (wild-type RIKEN strain). The maintenance and breeding conditions were kept the same as described in the 1.2.2 section of Chapter I.

2.2.3. Chemical treatments

To investigate the *sult2st3* expression during different developmental stages in RIKEN strain zebrafish, embryos were treated with TES (0.01-100 nM) alone at 48, 72, and 96 h postfertilization (hpf) for 24 hours.

Then 96 hpf was chosen as the measuring endpoint, the same as Chapter I. To analyze gene expression, embryos were exposed to 1-nM TES and 10-nM E2 alone or in combination with each of BPs, i.e., BPA, BPF, 2,2′-BPF, BPAF, BP C2, BPE, BPB, BPS, BPZ, and Bis-MP, with concentrations ranging from 0.001-100 μM. A vehicle control of 0.1% DMSO was also included. The exposure methods have been described in 1.2.3 section of Chapter I. All chemicals were diluted 1000-fold in E3 embryo medium to achieve the desired exposure concentrations, which were selected based on the previous evidence of efficacy. After 24 hours of incubation at 28.5°C, the samples were collected into MagNa Lyser Green Beads (Roche, Basel, Switzerland) for further analysis.

To assess morphological changes induced by each BP, embryos were exposed to DMSO or serial concentrations of BPA, BPE, BPF, BPAF, BP C2, and Bis-MP at 72 hpf and assessed phenotypic changes at 96 hpf. Each group includes 3 separate treatments and each treatment contains 10 embryos.

To assess the involvement of ER antagonist ICI, embryos were co-exposed to ER antagonist ICI and each of BPs. Each group includes 5 separate treatments and each treatment contains 10 embryos.

2.2.4. Gene expression measured by quantitative real-time PCR

The procedure of total RNA isolation, cDNA syntheses, and quantitative real-time PCR (qPCR) were described in the 1.2.4 section of Chapter I. In the present Chapter, *sult2st3* and *CYP19A1b* were measured and *eef1a1l1* was used as a housekeeping gene. The primer of *CYP19A1b* (forward, 5′-ACTAAGCAAGTCCTCCGCTGTGTACC-3′; reverse, 5′-TTTAAACATACCGATGCATTGCAG ACC-3′) was cited from Mouriec et al. (2009). The relative expression level of target genes was normalized to *eef1a1l1* as described in the 1.2.4 section.

2.2.5. In silico homology modelling and docking simulation

In silico analysis for anti-androgenic binding of ligands to zfAR was described in our previous study (Chen et al., 2023).

For anti-estrogenic binding potential prediction, the homology models of zebrafish ER (zfERα, zfERβ1, and zfERβ2) LBDs were constructed using the molecular simulation software MOE. The docking simulations and interactive energies of ligands to LBDs of zfERs were analyzed.

To construct a homology model, the amino acid sequence information for zebrafish ERs (zfERα, zfERβ1, and zfERβ2) was obtained from the National Center for Biotechnology Information (https://www.ncbi.nlm.nih.gov) with the following protein accession numbers: NP_694491 for zfERα, NP_777287 for zfERβ1, and NP_851297 for zfERβ2. The target sequences selected for modeling were the LBDs of these proteins. The homology models for the LBDs of zfERα, zfERβ1, and zfERβ2 were constructed based on the crystal structures of human ERα (PDB code: 3UUC) and human ERβ

(PDB code: 1L2J) retrieved from the Protein Data Bank (http://www.rcsb.org). The crystal structure of 3UUC is bound with BP C2 and 1L2J is bound with (R,R)-5,11-cis-diethyl-5,6,11,12-tetrahydrochrysene-2,8-diol (RR-THC). The MOE homology program (Delfosse et al., 2012; Möcklinghoff et al., 2010) was used for the construction of the models.

During the construction process, water molecules from the crystal structures of human ERs (hERs) were excluded, and structural defects and atomic collisions were adjusted using the Structure Preparation module within MOE. The Protonate 3D module was used for hydrogenation, and the AMBER10: EHT force field was employed to minimize the energy and optimize the structure of the hERs.

The optimized structures of human ERs were then utilized as templates for homology modeling of zfERs. The amino acid sequence of each zfER and its corresponding template structure were analyzed using the Protein Contacts program to identify conserved residue structures and gap positions. A total of 10,000 structures were generated for each zfER, incorporating 100 side chain samples for every 100 main chain models. The "induced fit" option was employed to adapt the ligand to the template structure during this process. The AMBER10:EHT force field and Born solvent-effect energy were utilized for structure prediction, while the generalized Born/volume integral (GB/VI) model parameters (Labute, 2008) were applied to generate the final model structures. The overall geometric and stereochemical quality of each model was assessed using Protein Geometry. To refine the zfER homology models, the phi (φ) and psi (ψ) twist angles of all amino acid residues and atomic collisions were confirmed by Ramachandran plots and adjusted through energy minimization. The resulting refined structures were considered as the final models for the docking simulation of endocrine disruptors.

To perform the molecular docking simulation of ligands to zfERs, the MOE's Induced Fit Docking feature within MOE software was employed. Before conducting the docking analysis, the

structure of the ligands, i.e., anti-estrogen (R,R)-cis-diethyl tetrahydro-2,8-chrysenediol (RR-THC), BPA, and its analogs, were constructed, and their geometry optimization was carried out using Rebuild3D with the AMBER10:EHT force field. These optimized structures were then compiled into a three-dementional (3D) structure database. In the docking simulation process, the ligand molecules were initially removed from the zfER LBD homology models. The MOE Site Finder module was utilized to identify the potential binding sites for each zfER LBD. For each prepared ligand, a total of 50 checks were performed using the default systematic search parameters employing Triangle Matcher. Two recording functions were used to measure the binding interactions, namely the London dG for rescoring the placement and the GBVI/WSA dG for rescoring the refinement. The most stable binding modes between the ligands and each zfER LBD were determined based on the lowest S-score (kcal/mol), calculated by the Dock program.

2.2.6 Morphological assessments

The morphological assessments were conducted for embryos exposed to BPA, BPE, BPF, BP C2, BPAF, and Bis-MP alone or in combination with ICI at 96 hpf, concentrating on the level of pericardial edema and blood flow reduction. The scoring methods were described in the section 1.2.6.

2.2.7 Statistical analysis

The difference analysis between chemical exposure groups and DMSO control group were determined by One Way ANOVA with Dunnett test post-hoc. Other methods, such as concentration-response of inhibition and morphological data analysis, were described in section 1.2.7.

2.3. Results

2.3.1. Anti-androgenic potency of BPA and its analogs in vivo

To confirm the expression profile of androgen responsive gene *sult2st3,* RIKEN embryos treated with TES (0.01-100 nM). *Sult2st3* was concentration-dependently induced by TES at 72 hpf, 96 hpf and 120 hpf (Fig. 9). At 72 hpf, TES induced a mild expression with EC_{50} of 0.53 nM and E_{max} of 1.5. In contrast, TES dramatically upregulated *sult2st3* expression level with EC_{50} of 0.37 nM and E_{max} of 4.5 at 96 hpf and EC_{50} of 0.31 nM and E_{max} of 4.1 at 120 hpf. Therefore, we chose 72-96 hpf as the exposure window to evaluate the anti-androgenic potentials of BPA and its analogs.

We analysed the mRNA expression level of *sult2st3* for the embryos exposed to TES alone or in combination with BPs by qPCR (Fig. 10). BPA, BPAF, BPE, BPF, and BPB showed anti-androgenic potentials in a concentration-dependent manner with the IC_{50} of 0.53, 3.7, 4.7, 12, and 87 μM, respectively. BP C2, 2,2′-BPF, and Bis-MP also exhibited anti-androgenic effect on the higher concentrations tested, even though no IC_{50} could be calculated. However, BPZ or BPS showed weak or no anti-androgenic potential. IC_{50} value suggests the order of anti-androgenicity as BPAF > BPE > BPA> BPF > BPB.

2.3.2. Anti-androgenic binding potentials of BPA and its analogs in silico

As shown in Fig. 11, 12, and Table 4, the positive control hydroxyflutamide formed two hydrogen bonds with amino acid Asn655 and Arg702 in zfAR LBD. BPE, BPF, BPB, BP C2, and BPS formed hydrogen bonds with amino acid Asn655 and Gln661. Besides, BPS formed one more hydrogen bond with Met737 and BP C2 formed a halogen bond with Met692 (Cl). Similar to these BPs, BPAF formed a hydrogen bond with Gln661 and a CH-π bond with Met695; 2,2′-BPF formed a hydrogen bond with Gln661 and a CH-π bond with Leu654. Differently, BPA, Bis-MP, and BPZ

form a hydrogen bond with Met695, Met737, and Met737, respectively, and BPA formed a CH-π bond with Met692.

Hydroxyflutamide has the lowest interaction energy of −8.22 kcal/mol among these ligands (Table 4). Among tested BPs, Bis-MP has the lowest interaction energy (−7.70), followed by BPE (−7.08), BPS (−7.05), BPB (−6.96), BPA (−6.92), BP C2 (−6.87), BPZ (−6.87), BPAF (−6.77), BPF (−6.47), and 2,2′-BPF (−6.35), indicating that Bis-MP has the strongest binding affinity to zfAR, followed by others in the order of interaction energy values from lower to higher.

2.3.3. Anti-estrogenic potentials of BPA and its analogs in vivo

As shown in Fig. 13, BP C2 reduced the E2-induced *CYP19A1b* expression in a concentration dependent manner. However, BPAF, BPA, BPF, BPB, and Bis-MP showed anti-estrogenic potentials with concentration-independent manner. For more details, BPAF significantly showed a repression effect on E2-induced *CYP19A1b* expression at 0.1 and 10 μM. BPA and BPF reduced the *CYP19A1b* induction at the highest concentration tested, 30 and 100 μM, respectively. BPB reduced the induction of *CYP19A1b* by E2 at 1 and 30 μM. Bis-MP significantly repressed E2-induced *CYP19A1b* expression at most of the tested concentrations. BPE and 2,2′-BPF showed no significant effects on E2-induced *CYP19A1b* expression. In contrast, BPZ and BPS potentiated the E2-induced *CYP19A1b* expression.

2.3.4. Anti-estrogenic binding potentials of BPA and its analogs in silico

In zfERα LBD (Fig. 14, 15, Table 5), RR-THC formed three hydrogen bonds with Met317, Glu321, and Arg362 on one side of phenyl rings and formed two CH-π bonds with Leu352 and Phe372. BPA, BPF, BP C2, and BPS formed two hydrogen bonds with Glu321 and Thr315 on both

sides of phenyl rings, respectively. Similarly, BPB and Bis-MP formed a hydrogen bond with Thr315 on one side and formed a hydrogen bond with Leu355 in another side. These BPs also formed a CH-π bond with Leu355 or Phe372. BPAF, BPE, and BPZ formed a hydrogen bond with Glu324 in one side. In addition, BPAF formed two CH-π bonds with Leu355 and Phe372 and BPE formed one CH-π bond with Phe372. The interaction energy order is RR-THC (−8.14) < Bis-MP (−7.73) < BPZ (−7.30) < BPB (−7.17) < BP C2 (−7.08) < BPAF (−6.92) < BPA (−6.90) < BPS (−6.86) < BPE (−6.66) < BPF (−6.33) < 2,2′-BPF (−5.93).

With the exception of 2,2′-BPF, one side of phenyl rings of RR-THC and all BPs formed a hydrogen bond with Glu338 in zfERβ1 LBD (Fig. 16, 17, Table 6). BPE, BP C2, and BPS formed a hydrogen bond with Met328 on another side of phenyl rings. RR-THC and BPB also formed a CH-π bond with Phe389, but BPS formed a CH-π bond with Leu372. The interaction energy order is RR-THC (−9.53) < Bis-MP (−8.12) = BPZ (−8.12) < BPB (−7.31) < BPAF (−7.30) < BP C2 (−7.06) < BPA (−6.96) < BPS (−6.78) < BPE (−6.75) < BPF (−6.57) < 2,2′-BPF (−6.35).

In zfERβ2 LBD (Fig. 18, 19, Table 7), RR-THC and most of BPs (except for BPB and 2,2′-BPF) formed a hydrogen bond with Glu323 on one side of phenyl rings. On another side of phenyl rings, BPB, BP C2, Bis-MP, BPZ, and BPS formed a hydrogen bond with Gly491. Besides, RR-THC formed two CH-π bonds with Leu357 and Phe374; BPE and BPB form a CH-π bond with Phe374; BPAF, 2,2′-BPF, and Bis-MP form a CH-π bond with Leu354, 357, and 316, respectively; BPA formed a CH-π bond with Ala320. The interaction energy order is RR-THC (−9.84) < Bis-MP (−8.33) < BPZ (−7.99) < BPAF (−7.72) < BPB (−7.63) < BP C2 (−7.31) < BPA (−7.14) < BPS (−6.93) < BPE (−6.81) < BPF (−6.33) < 2,2′-BPF (−6.30).

We further analysed the relationships of S-score obtained from *in silico* docking simulation between each of zfER subtypes, as well as relationships between S-score and the logarithmic n-octanol/water partition coefficient (log Kow) values (octanol-water partition coefficient) of ligands

(Fig. 20, 21). The S-scores between each of zfER subtypes showed significant positive correlation, implying the similar binding affinity of ligands to different ER subtypes. However, the S-scores and log Kow values showed significant negative correlations, suggesting that the more lipophilic the chemical is, the stronger binding affinity the chemical has.

2.3.5. Cardiovascular toxicity induced by BPA and its analogs

BPA, BPE, and BPF caused significant incidences of pericardial edema and blood flow reduction in zebrafish embryos at concentrations of 30 μM or 100 μM. However, BP C2, Bis-MP, and BPAF caused significant cardiovascular toxicity at lower concentrations (10 μM or lower) than BPA, BPE, and BPF (Fig. 22).

2.3.6. ICI effects on BPA and its analogs induced cardiovascular toxicity

As shown in Fig. 23, co-exposure with ER antagonist ICI could not reduce the incidences of pericardial edema and blood flow reduction induced by BPA, BPE, and BPF. Conversely, ICI worsens both pericardial edema and blood flow reduction caused by BPA. However, ICI reduced these malformations induced by BP C2, Bis-MP, and BPAF in a concentration-dependent manner, and almost reached 100% reduction at 80 μM.

2.4. Discussion

In the present study, all tested BPs showed anti-androgenic effects except for BPZ and BPS (Fig. 10), meanwhile BPAF, BPA, BPF, BPB, BP C2, and Bis-MP displayed anti-estrogenic effects in zebrafish embryos (Fig. 13). All BPs showed binding affinity and at least formed one hydrogen bond with amino acid residue in zfAR LBD (Fig. 11, 12, and Table 4). The similar results happen in zfER

subtypes, but 2,2′-BPF didn't form any bonds in zfERβ1 and only formed a CH-π bond in zfERβ2. Furthermore, some BPs, such as BP C2, Bis-MP, and BPAF, showed stronger cardiovascular toxicity than BPA, BPE, and BPF (Fig. 14-19, Table 5-7).

A numerous *in vitro* study reported the anti-androgenic activity potency of BPA and its analogs. About two decades ago, the anti-androgenic activity of BPA has been certified by inhibiting the androgenic activity of 5α-dihydrotestosterone with IC_{50} of 0.75 μM in an hAR reporter assay using African monkey kidney cell line CV-1 (Xu et al., 2005). An hAR reporter assay in PC-3-androgen receptor-luciferase-MMTV cells reported that BPA and BPF acted as full antagonists of hAR, and BPS showed no anti-androgenic activity (Molina-Molina et al., 2013). Meanwhile, BPA and BPS acted as weak hAR agonists (Molina-Molina et al., 2013). The androgenic activity of the androgen dihydrotestosterone was inhibited by BPAF, BPB, BPA, BPF, and BPS with IC_{50} of 1.3, 1.7, 4.3, 12, and 17 μM, respectively, in NIH3T3 cell transfected with the AR reporter gene (Kitamura et al., 2005). This indicates that the order of anti-androgenic activity among these BPs is BPAF > BPB > BPA > BPF > BPS. BPs also showed anti-androgenic activity in a yeast system with IC_{50} at the micromolar level following BP C2 > BPE > BPB > BPA > BPF (Conroy-Ben et al., 2018). Still, BPS and BPZ showed weak or no anti-androgenic activity, and BP C2 exhibited a slight androgenic activity (Conroy-Ben et al., 2018). In CHO-K1 cells transfected with a hAR assay, the antagonistic activities of BPA and its eight analogs were analyzed, revealing the following order of BPE > BPB > BPA > BPF > BPZ > bisphenol P (BPP) > bisphenol AP (BPAP) >> BPAF > BPS (weak or no activity) (Kojima et al., 2019). In another hAR yeast system, BPA and its analogs showed anti-androgenic activity in this order: BP C2 > BPAF > BPE = 2,2′-BPF > BPF = BPB > BPA > BPZ >> BPS (no activity) (van Leeuwen et al., 2019). Similarly, in another gene reporter cell line HELN-AR, BP C2 showed strongest anti-androgenic activity, followed by BPAF, BPA, BPB, BPE, BPF, and BPS (weak or no activity) (Delfosse et al., 2012). Generally, the anti-androgenic activities of BPA and above-

mentioned analogs (i.e., BP C2, BPAF, BPE, 2,2′-BPF, BPB, and BPF) showed anti-androgenic activity in different assay systems, but the potency order is different among systems. The biggest difference from the present study is the anti-androgenic potency of BP C2. In zebrafish, BP C2 showed anti-androgenic potential at the concentrations of 0.01, 1, and 10 μM, while it didn't show repression effects on TES-induced *sult2st3* expression at 0.001 and 0.1 μM (Fig. 13). Therefore, the IC_{50} value of BP C2 could not be determined to cause its weaker anti-androgenic potency than BPAF, BPE, BPA, BPF, and BPB. It is complex to compare the anti-androgenic potency of BPA and its analogs among different systems due to variations in experimental conditions and endpoints measured.

In a previous *in silico* study, BPBP showed the strongest binding affinity to hAR, followed by BPZ, BP C2, BPB, BPA, BPE, BPS, and BPF (Conroy-Ben et al., 2018). And their binding modes were similar to the AR agonist testosterone and the antagonist hydroxyflutamide, showing one phenyl ring of them always hydrogen-bonds with Thr877 and Asn705, while the other side bond with variable amino acids, such as Gln711, Cys784, and Ser778 (Conroy-Ben et al., 2018). In the present study, the binding affinity order of these BPs showed as BPE > BPS > BPB > BPA > BP C2 = BPZ > BPF (Table 4), which is different from the binding affinity for hAR. Hydroxyflutamide was hydrogen-bonded to Asn655 of zfAR in one side and hydrogen-bonded to Arg702 in another side (Fig. 11, 12, and Table 4). Similar to hydroxyflutamide, BPE, BPF, BPB, BP C2, and BPS, hydrogen-bonded to Asn655 in one side of phenyl rings, which means they showed anti-androgenic binding affinity as hydroxyflutamide. However, in another side of phenyl rings, these five bisphenols, BPAF, and 2,2′-BPF were hydrogen-bonded to Gln661, and BPA, Bis-MP, and BPZ were hydrogen-bonded to methionine residue at different position of zfAR LBD. Therefore, most BPA analogs tested in the present study were interacted to the same amino acid residue asparagine with zfAR at site 655. Additionally, Gln661, Met737, and Met695 may also be important for bisphenols to act as antagonists of zfAR.

Anti-estrogenic potentials of BPA and its analogs also have been discussed *in vitro* studies. In the MCF-7 reporter assay, the anti-estrogenic activities of BPA and nineteen related compounds were analyzed, where except TMBPA and TBBPA, all other compounds (e.g., BPAF, BPA, BPF, BPB, and BPS) showed no significant anti-estrogenic activity (Kitamura et al., 2005). In the CHO-K1 cell line, the anti-estrogenic activities to hERα and hERβ of nine bisphenols were analyzed, where BPAF and BPP showed antagonist activity with RIC_{20} of 5.4 μM and 1.1 μM for hERα and 8.0 μM and 0.93 μM for hERβ, respectively. In contrast, others, including BPE, BPA, BPF, BPB, BPZ, and BPS, showed no antagonist activity to both ERα and ERβ (Kojima et al., 2019). In an hERα yeast system, BPAF, BPE, BPA, BPF, BPB, BP C2, BPZ, and BPS showed negative anti-estrogenic activity and 2,2′-BPF showed a weak anti-estrogenic activity (van Leeuwen et al., 2019). However, in the present study, BPE, 2,2′-BPF, BPZ, and BPS could not inhibit E2-induced *CYP19A1b* expression, but BPAF, BPA, BPF, BPB, BP C2, and Bis-MP showed anti-estrogenic activity (Fig. 13).

According to Delfosse et al., bisphenols interact with hERα LBD via two binding modes, i.e., BPA-like agonist mode and BP C2-like antagonist mode (Delfosse et al., 2012). In their study, agonist mode BPA, like E2, hydrogen-bonded to amino acid residue Arg394 and Glu353 in one side and to His524 in another side, while antagonist mode BP C2 hydrogen-bonded to Thr347 in another side (Fig. 14, 15). Similarly, the agonist ligand binding affinities of BPA, BPAF, BPB, and BP C2 have been predicted in medaka (*Oryzia latipes*) and common carp (*Cyprinus carpio*) (Yamaguchi et al., 2015). In their study, BP C2 showed the most potent binding affinity, followed by BPAF and BPA for both medaka ERα and carp ERα, while the binding modes were different among the two species. That is, BP C2, BPAF, and BPA hydrogen-bonded to 2, 3, and 2 amino acid residues of medaka ERα, respectively, and to 1, 2, and 2 residues of carp ERα, respectively, but one phenyl ring of these compounds was bonded with Glu365 in ERα of both medaka and carp. In the present study, the antagonist modes of most bisphenols were hydrogen-bonded to Glu321 in zfERα and hydrogen-

bonded to Glu338 in zfERβ1 in one side of phenyl rings, which is similar to the agonist modes showed in our previous study (Kubota et al., 2023). However, in another side of phenyl rings, the agonist modes and antagonist modes were hydrogen-bonded to different residues. Hence, the ligand binding modes of BPA and its analogs exhibited variations in their agonistic and antagonistic properties across different ER subtypes and species.

However, it is worth noting that antagonist modes of bisphenols hydrogen-bonded one or two residues are all different with their agonist mode in zfERβ2 (Kubota et al., 2023). This implies that the binding mode of ligands to zfERβ2 may be used to distinguish estrogenic or anti-estrogenic potentials of ligands.

BPAF has been reported to have stronger developmental toxicity (e.g., decreased heart rate, cardiac edema, and spinal curve) and estrogenic potency in developing zebrafish than BPA, BPF, and BPS (Moreman et al., 2017; Mu et al., 2018). In addition to BPAF, the present study indicated that BP C2 and Bis-MP also showed stronger cardiovascular toxicity than BPA. Especially, BP C2 showed stronger toxicity than Bis-MP and BPAF. The co-exposure studies suggested that mechanisms of BPs-induced cardiovascular toxicity appear to differ among BPs. ER is unlikely to mediate cardiovascular toxicity caused by BPA, BPE, or BPF. However, further studies are needed to confirm the involvement of ER in BP C2-, Bis-MP-, and BPAF-induced cardiovascular toxicity.

2.5. Conclusion

BPA and all tested analogs showed anti-androgenic effects, with the exception of BPZ and BPS. On the other hand, BPAF, BPA, BPF, BPB, BP C2, and Bis-MP also exhibited anti-estrogenic effect. Amino acid residues Asn655, Gln661, Met695, and Met737 are potentially significant in determining the binding affinities of BPA and its analogs to zfAR. The binding modes of BPs are different between agonistic and antagonistic properties in all ER subtypes. Particularly, ERβ2 shows promise as a

potential marker for distinguishing agonists or antagonists. Agonistic modes of BPs are hydrogen-bonding with His494, whereas their antagonistic modes are hydrogen-bonding with Glu323 and Gly491. Moreover, BP C2, Bis-MP, and BPAF have stronger cardiovascular toxicity than BPA, BPE, and BPF. The cardiovascular toxicity induced by BPA, BPE, and BPF may not be mediated by ER signaling, but further studies are needed to confirm the (non)involvement of ER in developmental toxicity.

Table 3. List of chemicals used for *in vivo* exposure study and their predicted hydrophobicity.

Name of chemical	Log *K*ow	CAS#	Manufacturer	Purity
ICI	9.09	129453-61-8	Sigma-Aldrich	98
E2	4.01	50-28-2	Sigma-Aldrich	97
BPAF	4.47	1478-61-1	Wako Pure Chemical Industries	98
BPE	3.19	2081-08-5	Wako Pure Chemical Industries	98
BPA	3.32	80-05-7	Wako Pure Chemical Industries	99
BPF	2.91	620-92-8	Kanto Chemical	99
BPB	4.13	77-40-7	Tokyo Chemical Industry	98
BP C2	5.00	14868-03-2	Tokyo Chemical Industry	98
2,2'-BPF	3.06	2467-02-9	Sigma-Aldrich	98
Bis-MP	4.70	6807-17-6	Tokyo Chemical Industry	98
BPZ	5.48	843-55-0	Wako Pure Chemical Industries	98
BPS	1.65	80-09-1	Wako Pure Chemical Industries	98

Table 4. Interaction energies and key amino acid residues of ligands binding with the zfAR LBD.

Compound	S-score (kcal/mol)	Hydrogen bonding	CH-π
Hydroxyflutamide	−8.22	Asn655, Arg702	—
BPAF	−6.77	Gln661	Met695
BPE	−7.08	Asn655, Gln661	—
BPA	−6.92	Met695	Met692
BPF	−6.47	Asn655, Gln661	—
BPB	−6.96	Asn655, Gln661	—
BP C2	−6.87	Asn655, Gln661, Met692	—
2,2'-BPF	−6.35	Gln661	Leu654
Bis-MP	−7.70	Met737	—
BPZ	−6.87	Met737	—
BPS	−7.05	Asn655, Gln661, Met737	—

Table 5. Interaction energies and key amino acid residues of ligands binding with the zfERα LBD.

Compound	S-score (kcal/mol)	Hydrogen bonding	CH-π
RR-THC	−8.41	Met317, Glu321, Arg362	Leu352, Phe372
BPAF	−6.92	Glu321	Leu355, Phe372
BPE	−6.66	Glu321	Phe372
BPA	−6.90	Thr315, Glu321	Leu355
BPF	−6.33	Thr315, Glu321	Phe372
BPB	−7.17	Thr315, Leu355	Phe372
BP C2	−7.08	Thr315, Glu321	Phe372
2,2'-BPF	−5.93	—	Met356
Bis-MP	−7.73	Thr315, Leu355	—
BPZ	−7.30	Glu321	—
BPS	−6.86	Thr315, Glu321	Phe372

Table 6. Interaction energies and key amino acid residues of ligands binding with the zfERβ1 LBD.

Compound	S-score (kcal/mol)	Hydrogen bonding	CH-π
RR-THC	−9.53	Glu338	Phe389
BPAF	−7.30	Glu338	—
BPE	−6.75	Glu338, Met328	—
BPA	−6.96	Glu338	—
BPF	−6.57	Glu338	—
BPB	−7.31	Glu338	Phe389
BP C2	−7.06	Glu338, Met328	—
2,2'-BPF	−6.35	—	—
Bis-MP	−8.12	Glu338	—
BPZ	−8.12	Glu338	—
BPS	−6.78	Glu338, Met328	Leu372

Table 7. Interaction energies and key amino acid residues of ligands binding with the zfERβ2 LBD.

Compound	S-score (kcal/mol)	Hydrogen bonding	CH-π
RR-THC	−9.84	Glu323	Leu357, Phe374
BPAF	−7.72	Glu323	Leu354
BPE	−6.81	Glu323	Phe374
BPA	−7.14	Glu323	Ala320
BPF	−6.33	Glu323	—
BPB	−7.63	Gly491	Phe374
BP C2	−7.31	Glu323, Gly491	
2,2'-BPF	−6.30	—	Leu357
Bis-MP	−8.33	Glu323, Gly491	Leu316
BPZ	−7.99	Glu323, Gly491	—
BPS	−6.93	Glu323, Gly491	—

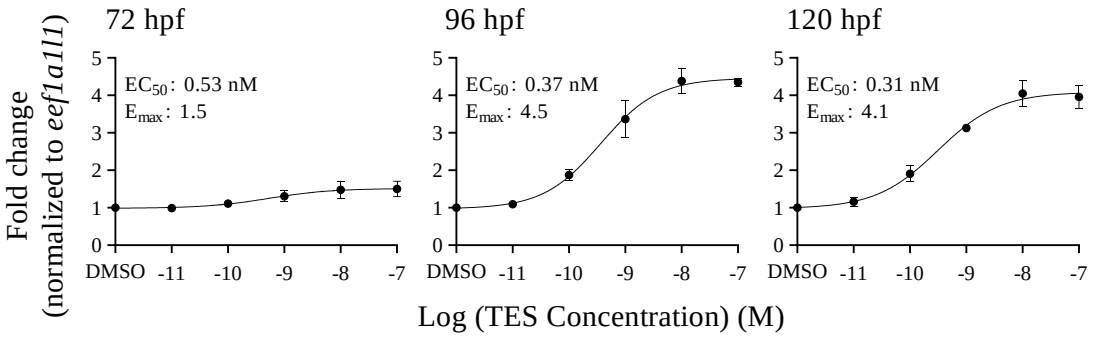

Fig. 9. Concentration-response relationships for the effects of TES on *sult2st3* mRNA expression in RIKEN zebrafish at the different developmental stages. Data points represent mean fold change values relative to the DMSO control with the SEM (n = 4).

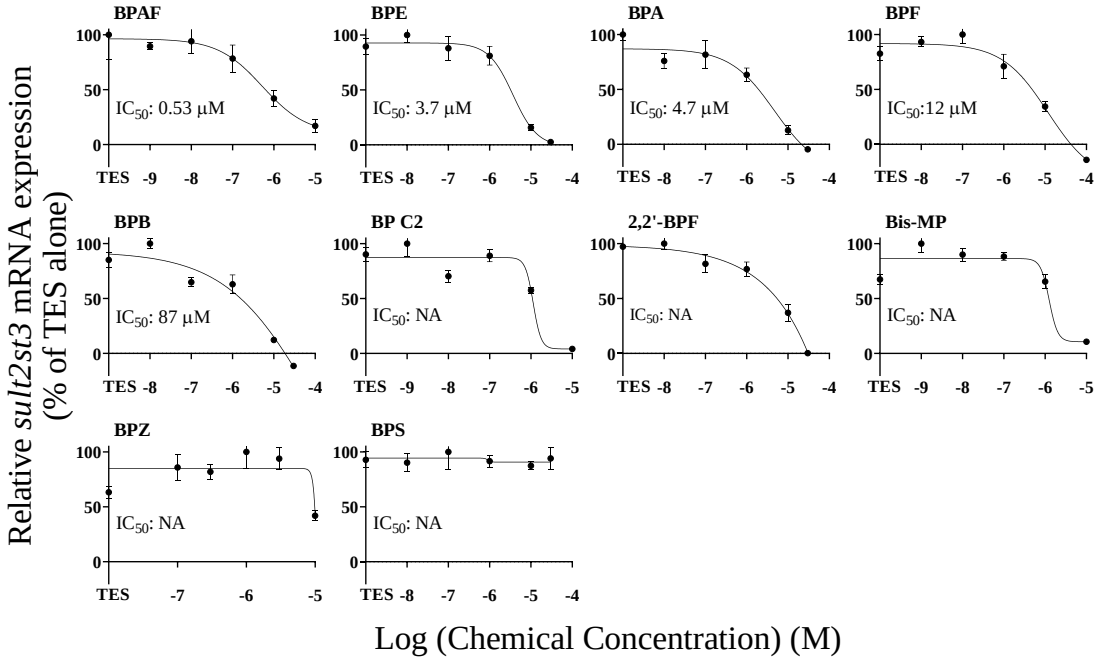

Fig. 10. Effects of BPA and its analogs on TES-induced *sult2st3* mRNA expression in zebrafish at 96 hpf. Data represent mean percentages of 1-nM TES-induced expression of *sult2st3* with SEM (n = 4).

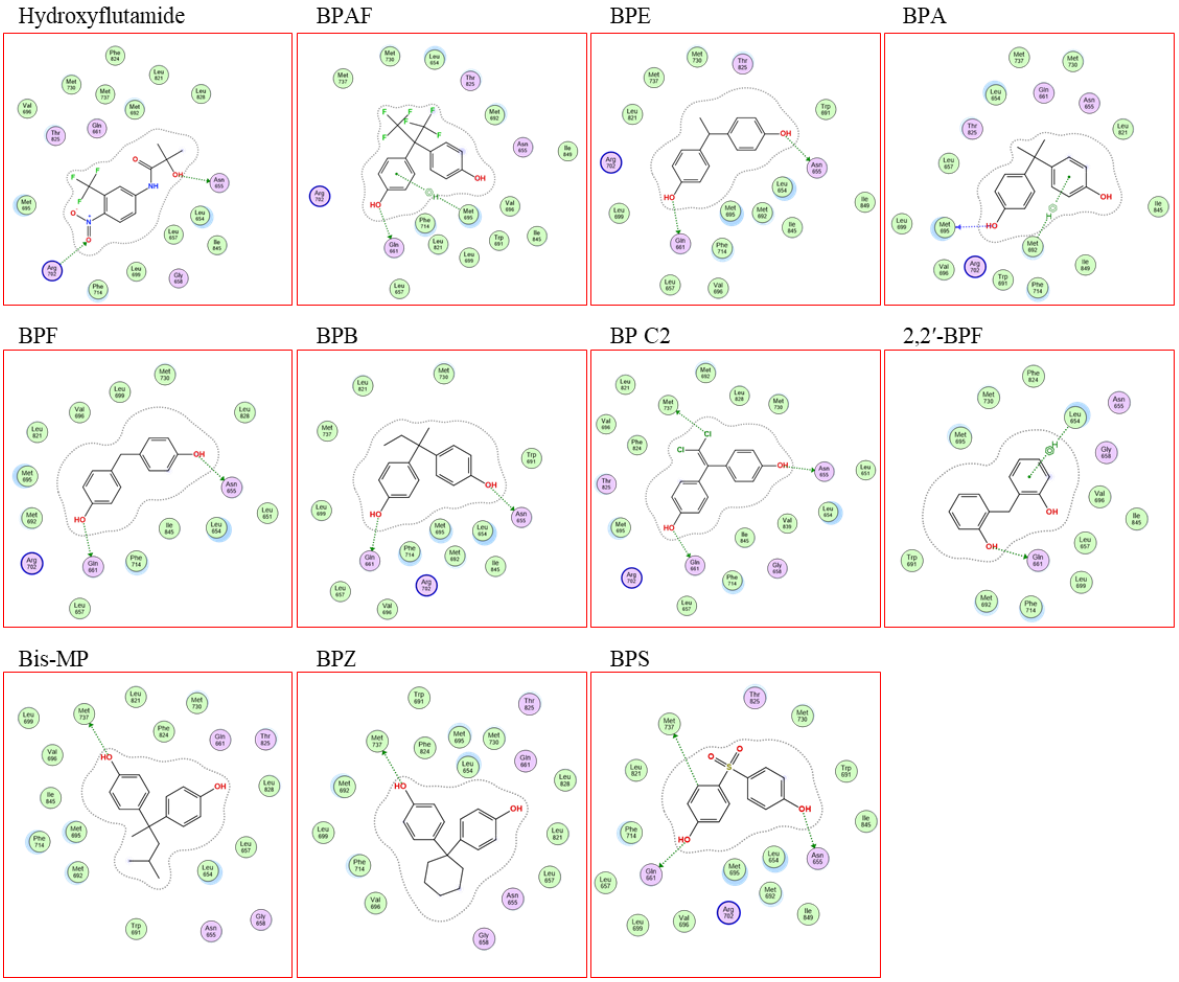

Fig. 11. Ligand interaction of hydroxyflutamide and tested bisphenols zfAR LBD. The dashed lines indicate specific interactions (hydrogen bonds or CH-π bonds) between the ligand and amino acid residues of zfAR LBD.

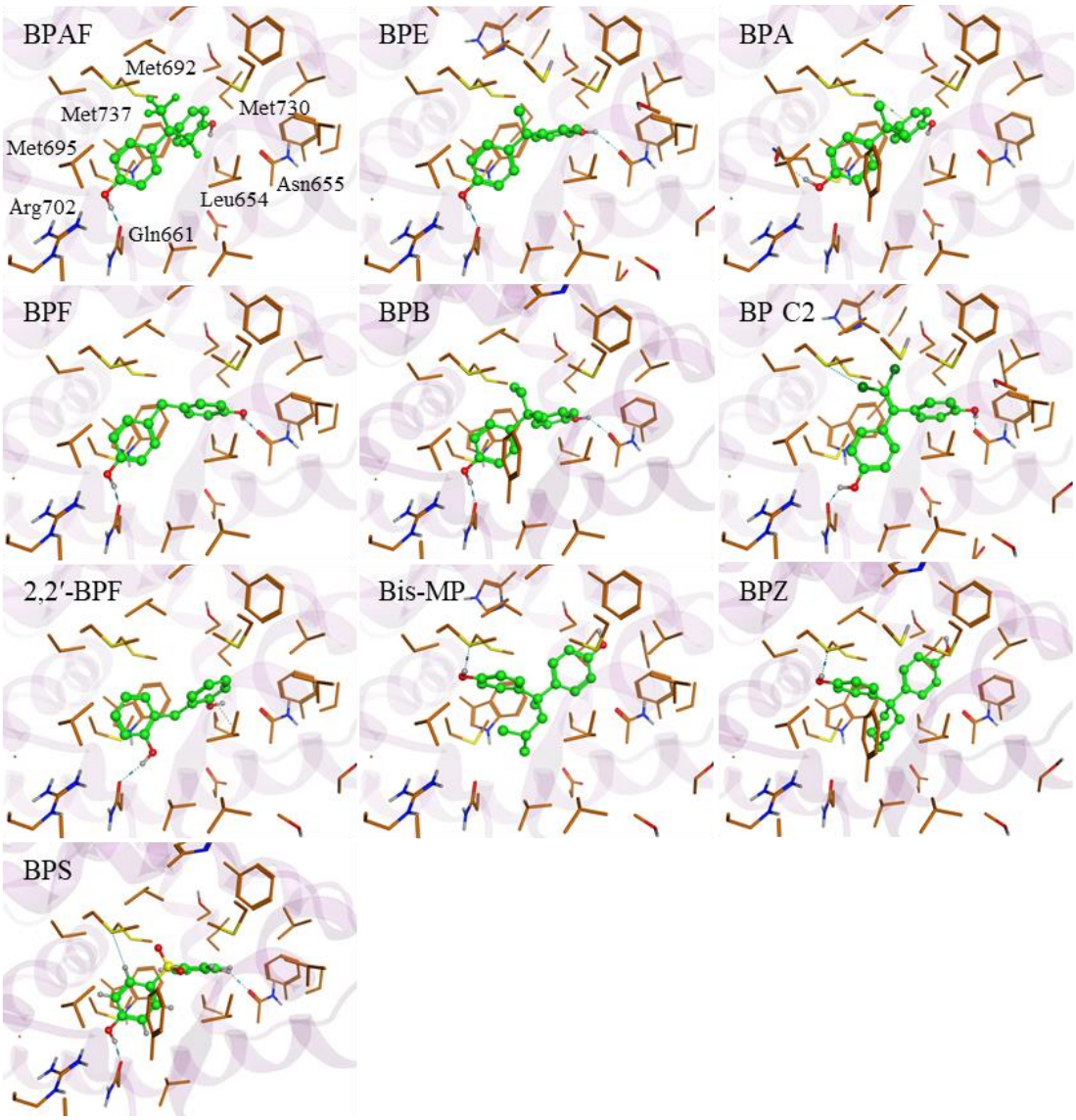

Fig. 12. Binding modes of hydroxyflutamide and tested bisphenols to the zfAR. The blue dotted line represents the hydrogen bonds, while the green dotted line represents the CH-π bonds. These lines indicate the specific interactions between the ligand and amino acid residues of zfAR LBD.

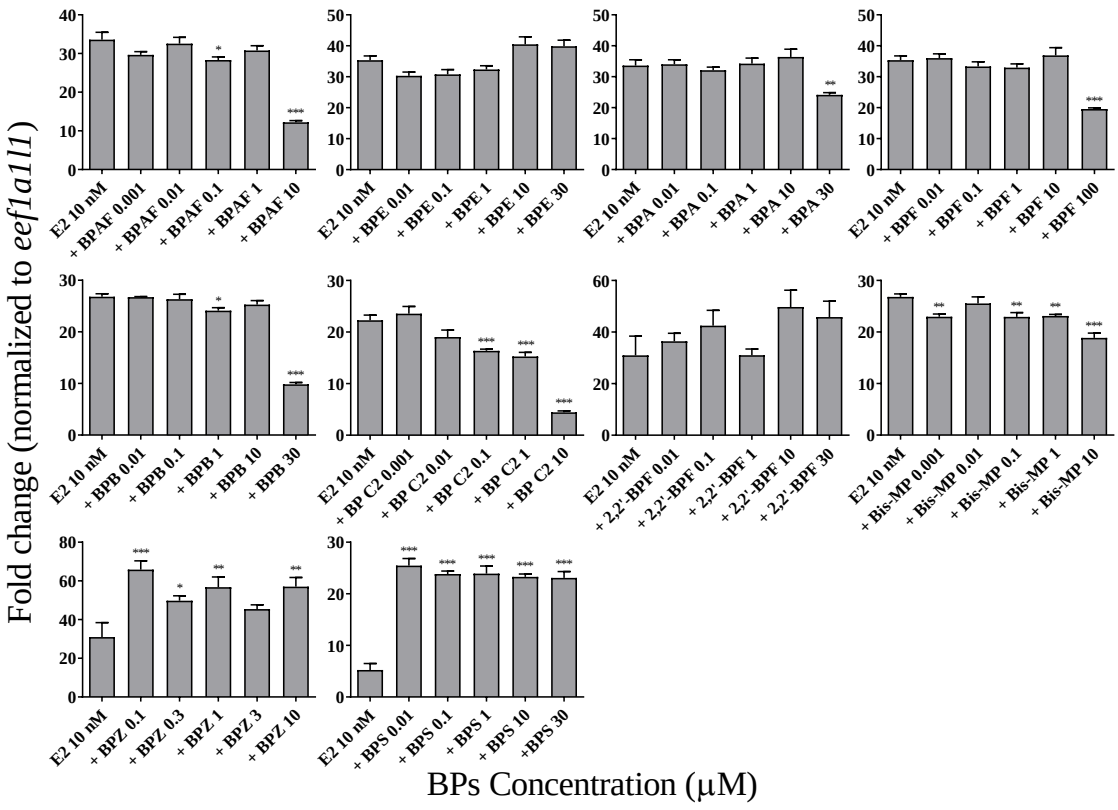

Fig. 13. Effects of BPA and its analogs on E2-induced *CYP19A1b* expression in zebrafish at 96 hpf. Data represent mean fold change values relative to the DMSO control (not show in the graphs) with the SEM (n = 4). * $P < 0.05$, ** $P < 0.01$, *** $P < 0.001$.

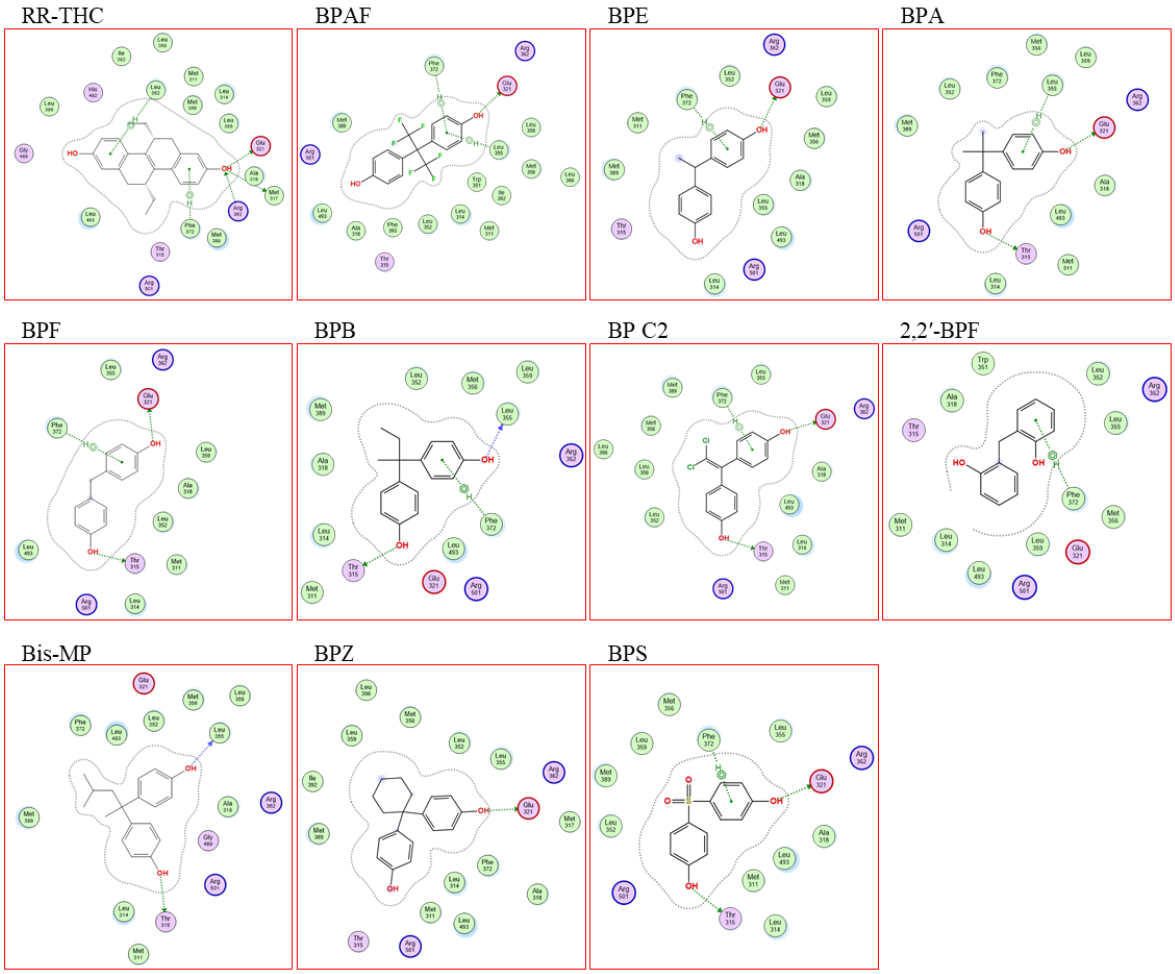

Fig. 14. Ligand interaction of hydroxyflutamide and tested bisphenols zfERα LBD. The dashed lines indicate specific interactions (hydrogen bonds or CH-π bonds) between the ligand and amino acid residues of zfERα LBD.

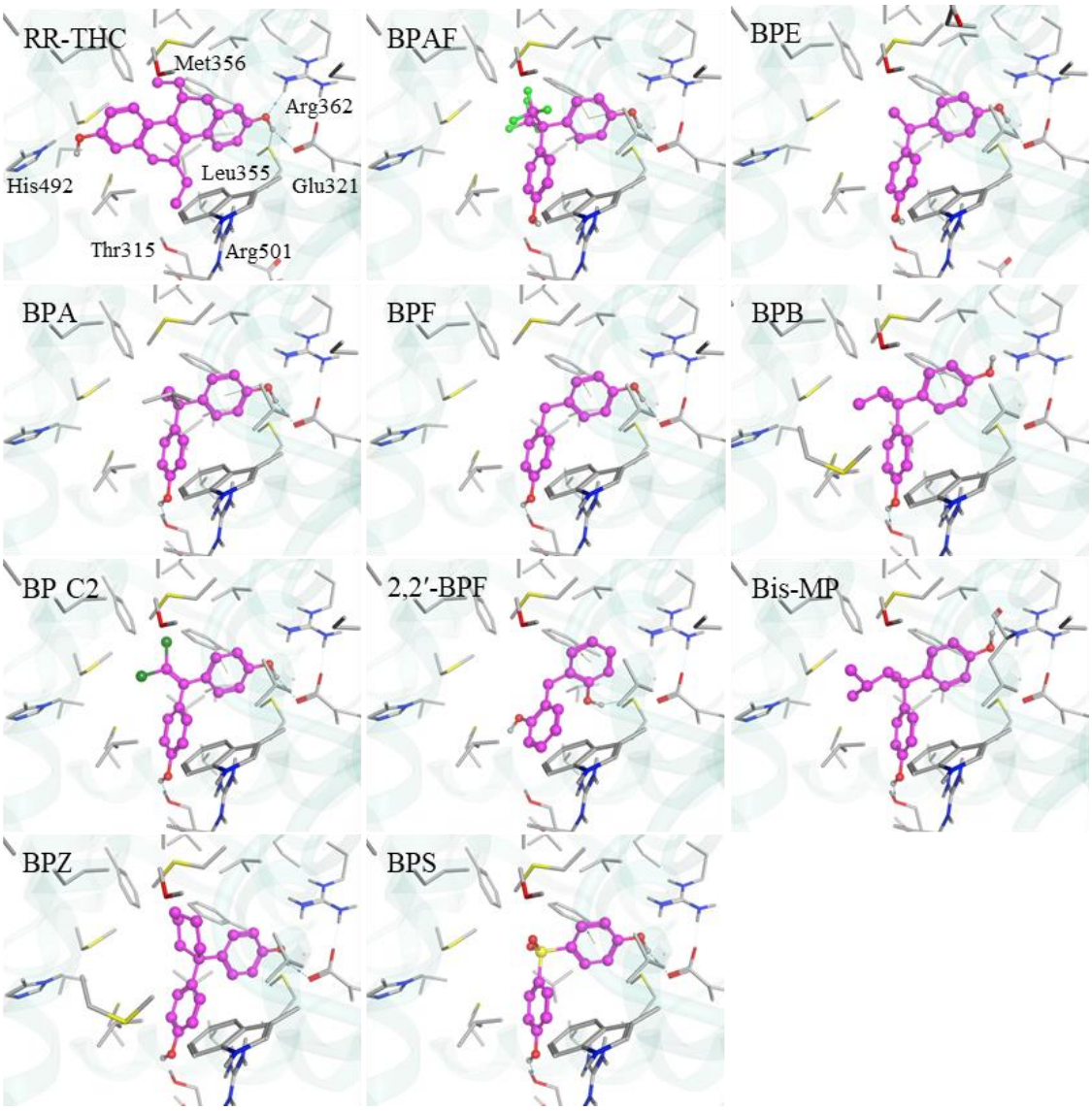

Fig. 15. Binding modes of RR-THC and tested bisphenols to the zfERα. The blue dotted line represents the hydrogen bonds, while the green dotted line represents the CH-π bonds. These lines indicate the specific interactions between the ligand and amino acid residues of zfERα LBD.

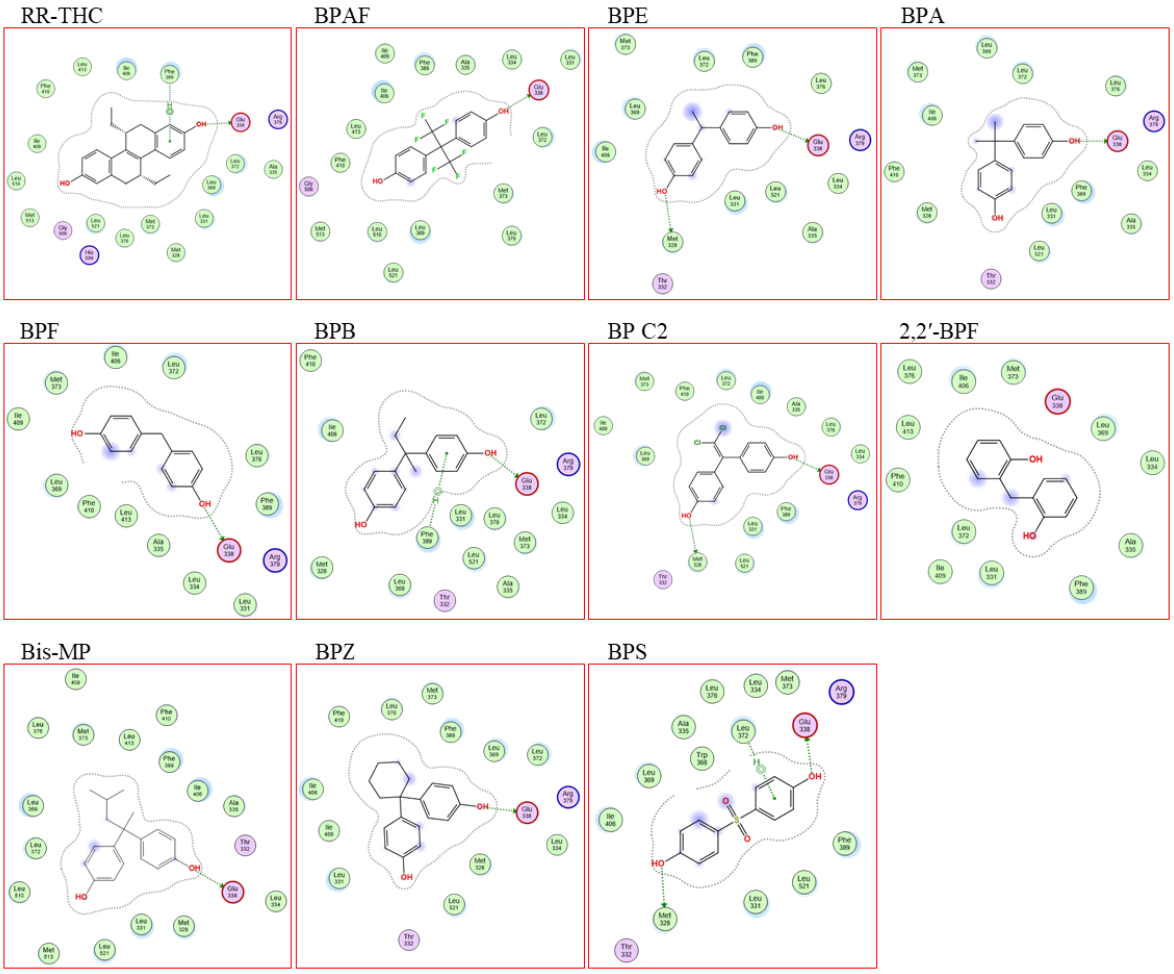

Fig. 16. Ligand interaction of hydroxyflutamide and tested bisphenols zfERβ1 LBD. The dashed lines indicate specific interactions (hydrogen bonds or CH-π bonds) between the ligand and amino acid residues of zfERβ1 LBD.

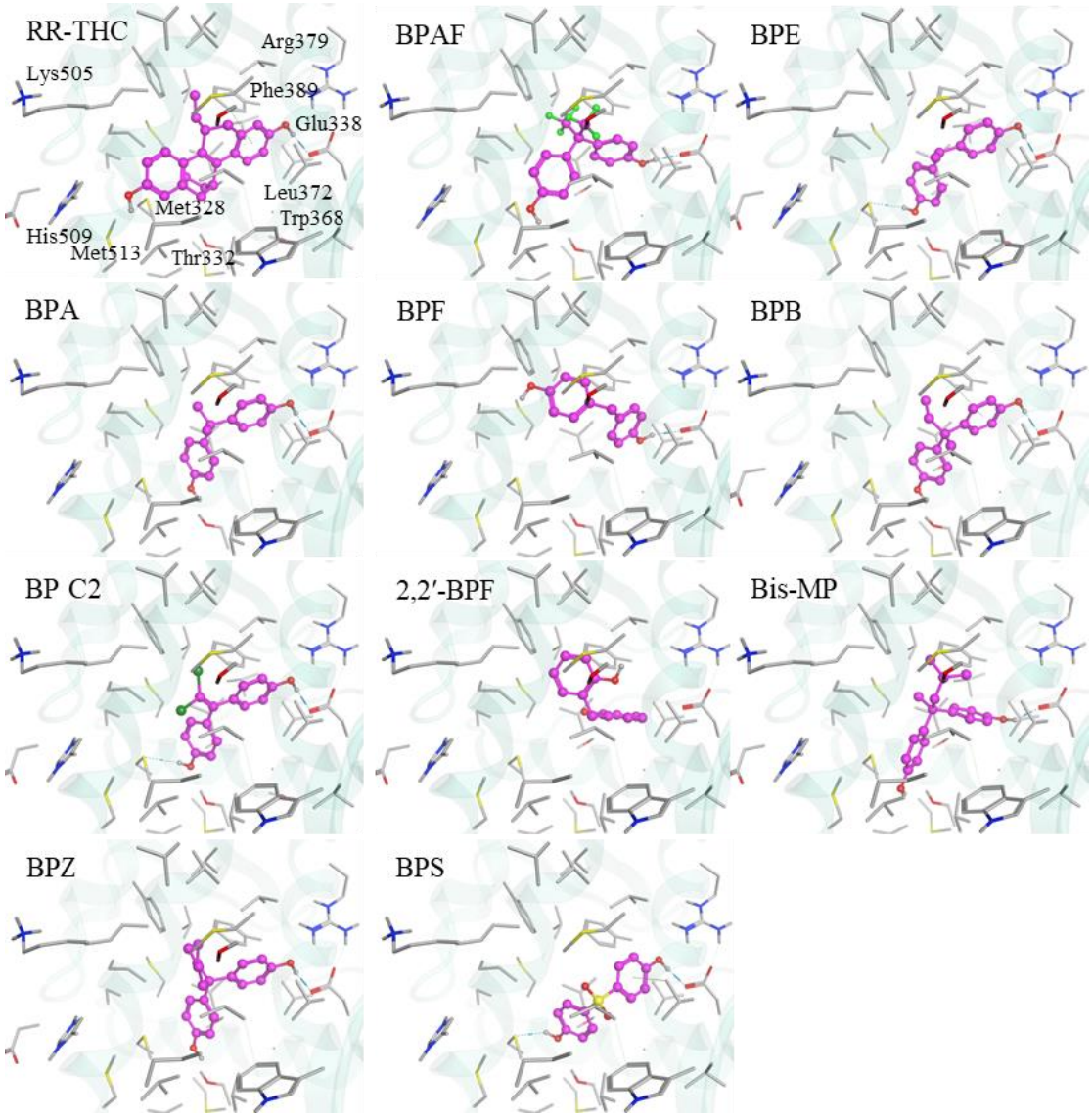

Fig. 17. Binding modes of RR-THC and tested bisphenols to the zfERβ1. The blue dotted line represents the hydrogen bonds, while the green dotted line represents the CH-π bonds. These lines indicate the specific interactions between the ligand and amino acid residues of zfERβ1 LBD.

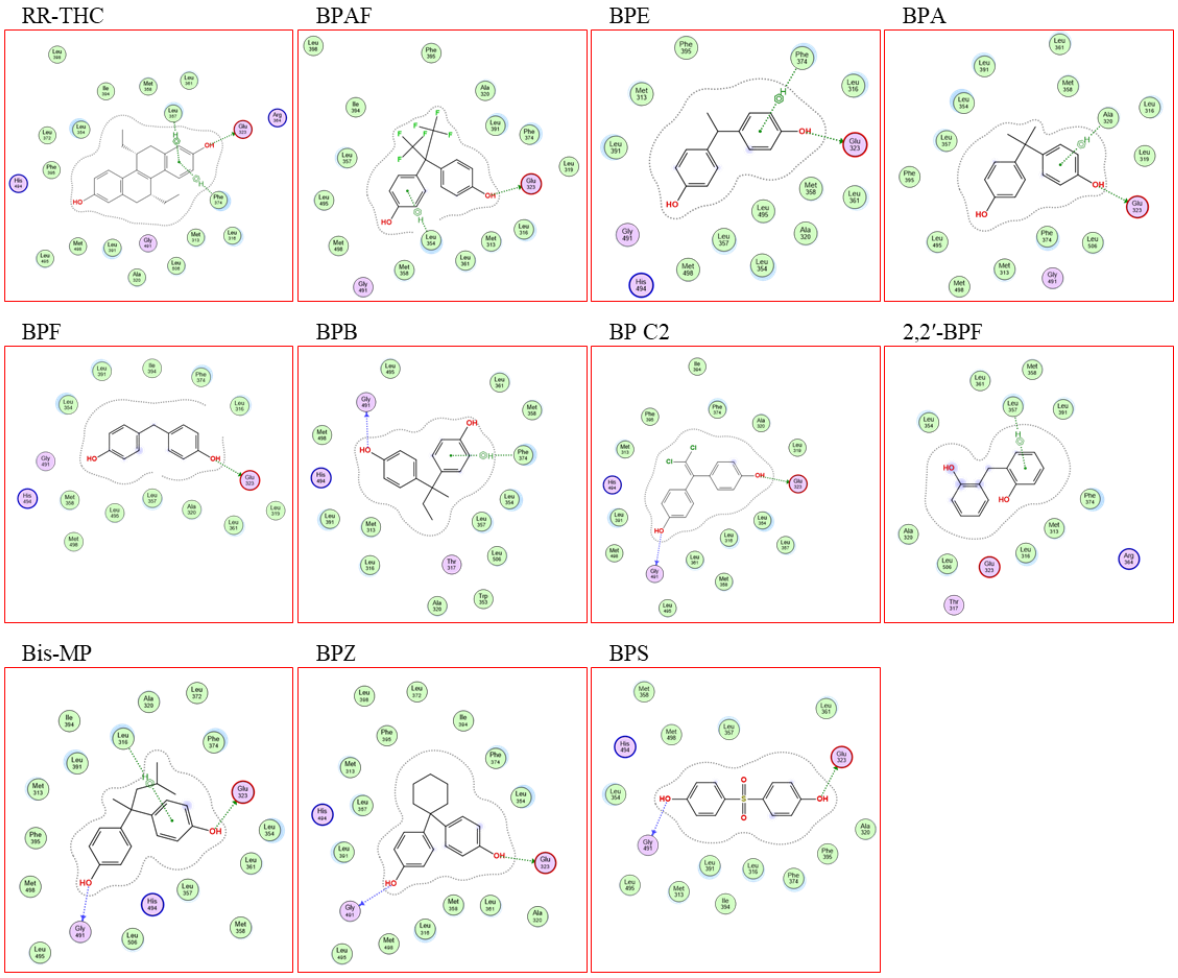

Fig. 18. Ligand interaction of hydroxyflutamide and tested bisphenols zfERβ2 LBD. The dashed lines indicate specific interactions (hydrogen bonds or CH-π bonds) between the ligand and amino acid residues of zfERβ2 LBD.

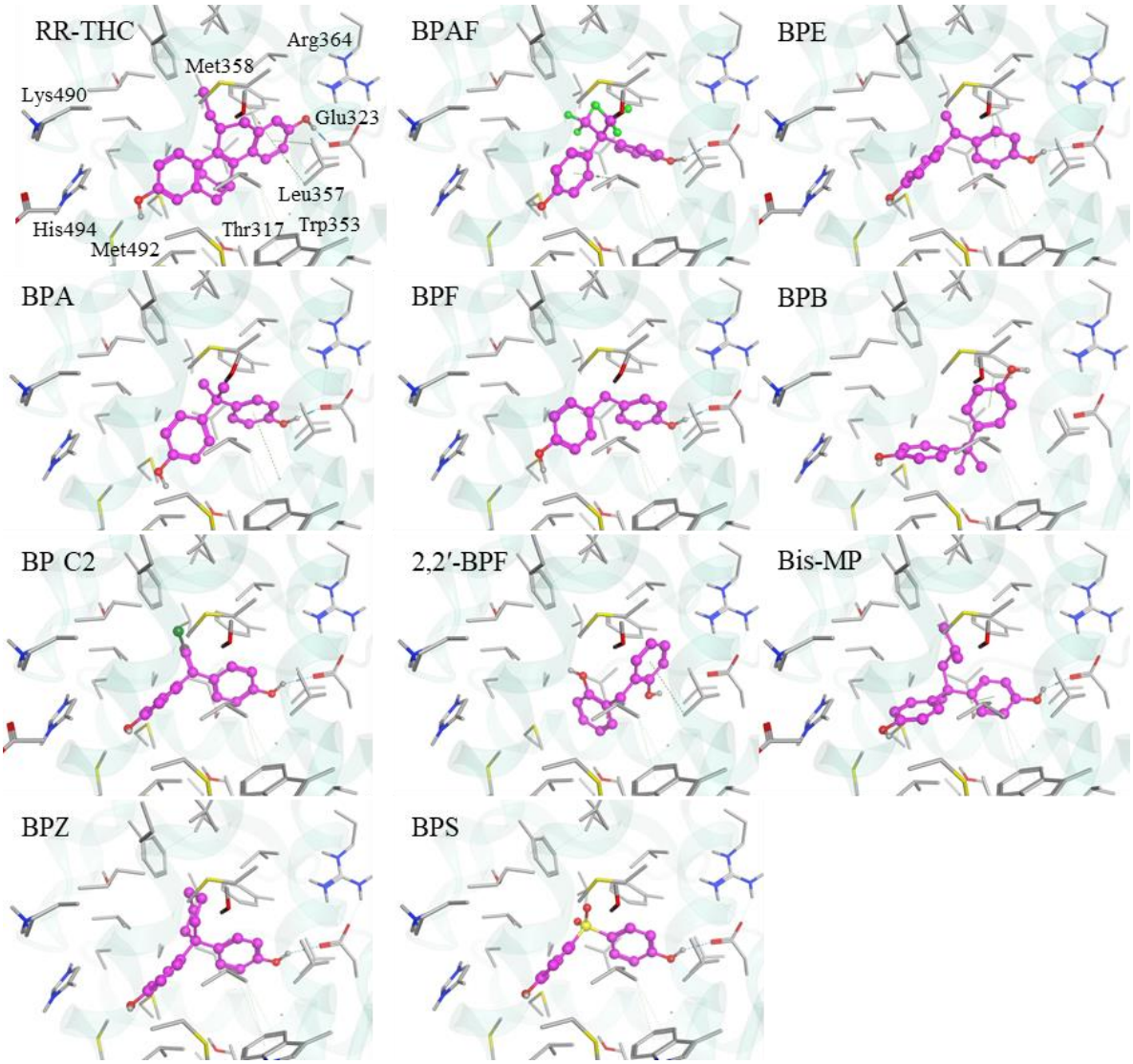

Fig. 19. Binding modes of RR-THC and tested bisphenols to the zfERβ2. The blue dotted line represents the hydrogen bonds, while the green dotted line represents the CH-π bonds. These lines indicate the specific interactions between the ligand and amino acid residues of zfERβ2 LBD.

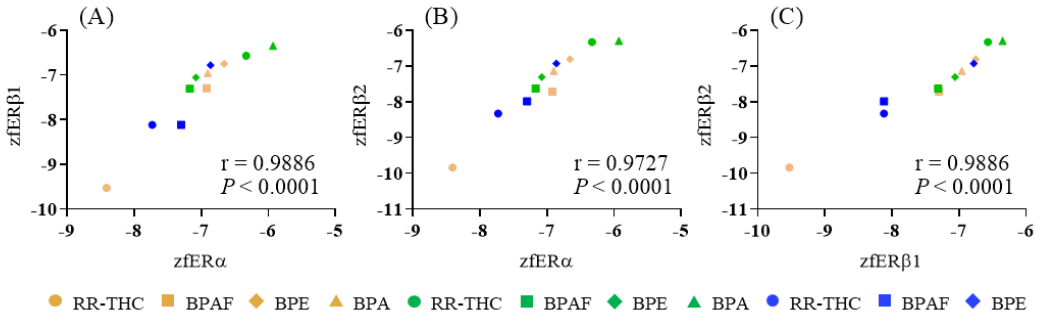

Fig. 20. Relationships between S-scores obtained from *in silico* docking simulation for RR-THC and BPs to each of ER subtypes. zfERα vs zfERβ1 (A), zfERα vs zfERβ2 (B), zfERβ1 vs zfERβ2 (C).

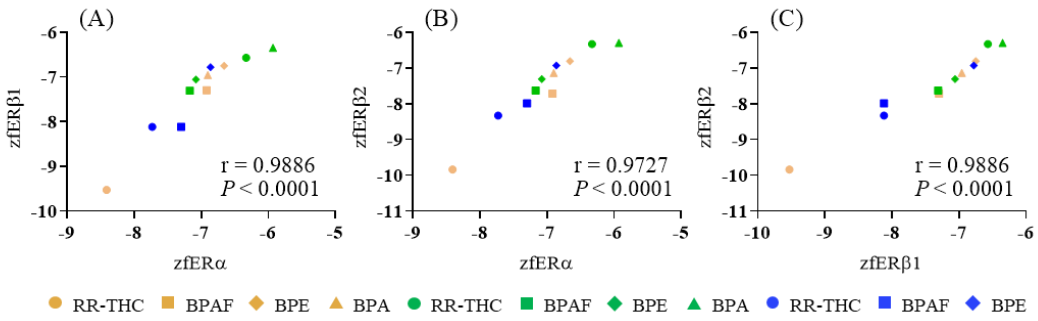

Fig. 21. Correlations between interaction energy of ligands to zebrafish ER subtypes and Log Kow values of RR-THC and BPs. Rho (r) and *P* values are from Spearman's rank correlation tests. zfERα (A), zfERβ1 (B), and zfERβ2 (C).

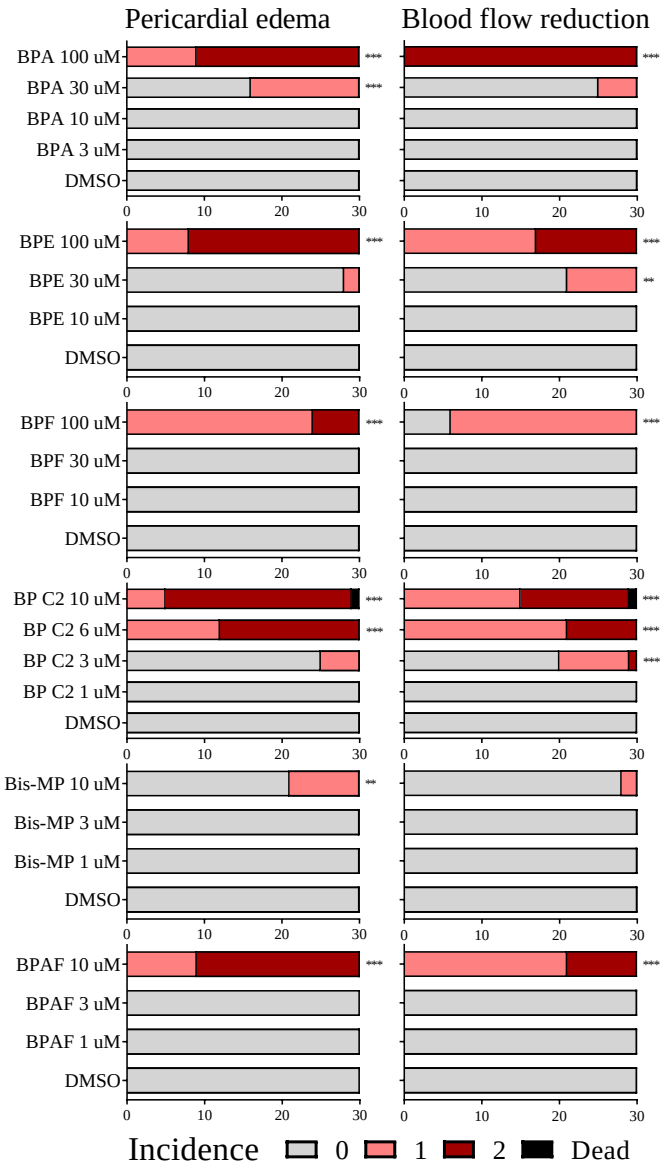

Fig. 22. Incidence of pericardial edema and blood flow reduction caused by BPA, BPE, BPF, BP C2, Bis-MP, and BPAF. Affected embryos were represented as mean number based on three separate experiments. Statistically significant differences in the numbers of affected and unaffected embryos between the DMSO and exposure groups were evaluated using Fisher's exact test for pairwise comparisons (** $P < 0.01$, *** $P < 0.001$, n = 30).

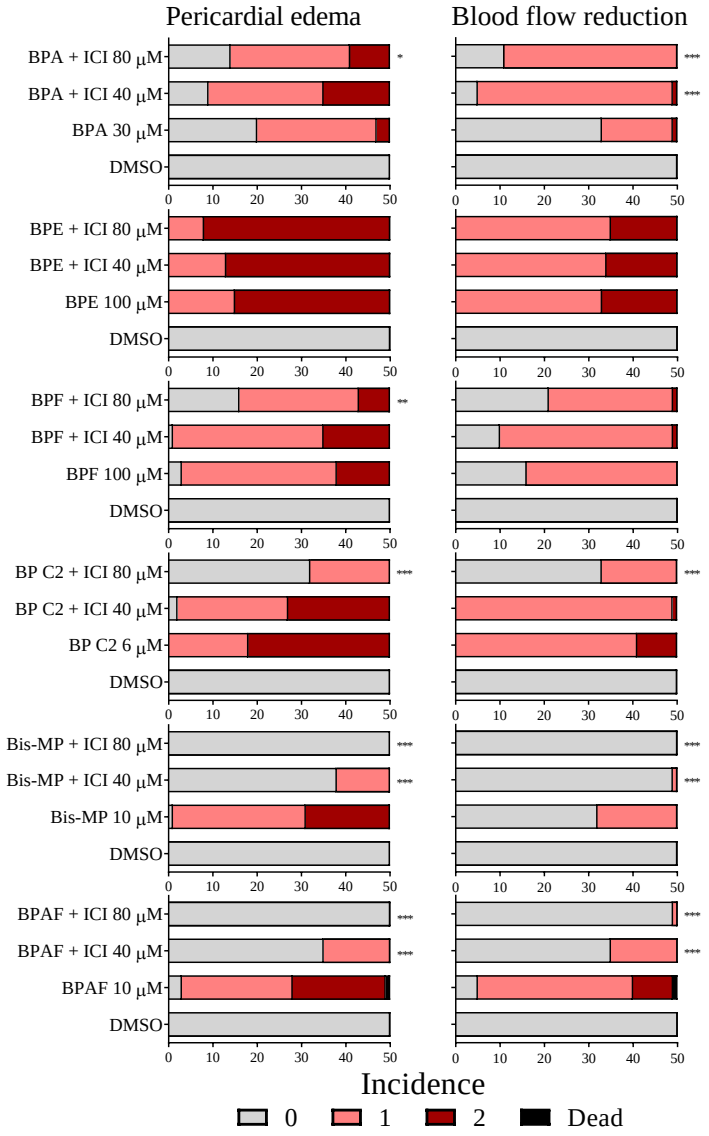

Fig. 23. Incidence of pericardial edema and blood flow reduction caused by BP alone or in combination with ICI. Affected embryos were represented as mean number based on five separate experiments. Statistically significant differences in the numbers of affected and unaffected embryos between BP exposure alone and co-exposure groups were evaluated using Fisher's exact test for pairwise comparisons (* $P < 0.05$, ** $P < 0.01$, *** $P < 0.001$, n = 50).

General Discussion

We measured the dose-response of TES-induced *sult2st3* mRNA expression in zebrafish embryos of the wild types AB strain and RIKEN strain. Similar to the AB strain zebrafish, the relative expression level of *sult2st3* at 72 hpf showed quite low induction in the RIKEN strain embryos exposed to TES. However, the relative expression level of *sult2st3* at 96 and 120 hpf were comparable induction in both zebrafish strains. These results indicate that the initiation stage of *sult2st3* mRNA expression is similar among zebrafish strains, thus the same optimal exposure window can be chosen.

Several zebrafish studies have demonstrated that exposure to BPA and its analogs disrupts normal development and reproductive system function (Cariati et al., 2019; Chen et al., 2016; Pelch et al., 2019). Notably, exposure to BPA alternatives such as BPAF and fluorene-9-bisphenol during the embryonic stage of zebrafish altered gene expression in spermatogenesis and meiosis, impairing gonadal development and reducing fertility in adult fish (Meng et al., 2023). The estrogenic and anti-androgenic potentials of BPA and its analogs (BPAF, BPB, BPE, and BPF) have been extensively investigated across various model systems (Chen et al., 2016). Furthermore, the anti-androgenic potential of tested pesticides (i.e., DDE, VIN, LIN, and FEN) has been identified in different systems, and their potency order differs among AR species. The variations in experimental conditions and endpoint measurements also caused the complex to compare the anti-androgenic potency of BPs. However, BPA and its analogs, e.g., BP C2, BPAF, BPE, 2,2′-BPF, BPB, and BPF, showed anti-androgenic activity in different assay systems even though their potency orders differ.

The ligand binding modes of the tested compounds to zfAR showed no clear tendency among pesticides and BPs. DDE, LIN, and FEN commonly bonded to Arg702, whereas BPA bonded to Met692 and Met695. Furthermore, most BPA analogs bonded to Asn655 and/or Gln661, and Bis-MP

or BPZ bonded to Met737. However, a larger number of additional cluster compounds need to be tested to draw a definitive conclusion.

The present study observed that antagonist modes of BPs hydrogen-bonded one or two residues which differ from the residues involved in their agonist mode, when interacting with zfERβ2. This suggests that zfERβ2 could serve as a marker to distinguish the agonistic or antagonistic characteristics of compounds. Furthermore, the detection of numerous contaminants in the environment, food containers, and other daily products emphasizes the importance of investigating their endocrine-disrupting toxicity, highlighting the ongoing significance of this research topic.

General Conclusion

The present study has established a fast and efficient quantitative assay system utilizing developing zebrafish to identify anti-androgens. We validated the ligand-binding affinity of the tested compounds using our *in silico* homology model. Our results indicate that Arg702 plays a key role in the binding of tested pesticides to zfAR, while Asn655 and/or Gln661 play important roles in the binding of most tested BPs to zfAR. Most of the tested BPs demonstrated both anti-androgenic and anti-estrogenic activities in zebrafish. The ligand binding affinity of BPs to ERs may not exhibit heterogeneity in terms of interaction energies between agonistic and antagonistic activities, but it does show diversity in binding modes. Specifically, in ERβ2, it could serve as a means to identify the agonistic and antagonistic activities of BPs. Notably, BPAF exhibited significantly stronger anti-androgenic potency than BPA. Moreover, BP C2, Bis-MP, and BPAF showed stronger cardiovascular toxicity than BPA, BPE, and BPF. The cardiovascular toxicity caused by BPA, BPE, and BPF was unlikely to be mediated by ER signaling, but further investigation is needed to confirm the involvement of ER in BP C2-, Bis-MP-, and BPAF-induced cardiovascular toxicity. The present study highlights the presence of potential risks in BPA-free products. Consequently, most BPA alternatives have not been sufficiently studied regarding their endocrine-disrupting and developmental toxicities.

Abstract

A significant and varied array of endocrine-disrupting chemicals (EDCs) has been released into the environment since World War II (Colborn et al., 1993). EDCs have the capacity to interfere with the normal functioning of the endocrine and reproductive systems by mimicking or impeding the actions of endogenous hormones. Hence, there is concern regarding the impact of EDCs on ecosystems, leading to the conduction of numerous studies from this perspective. Studies have reported that exposure to anti-androgens and estrogens are associated with the feminization of wild fish. Considering the reproductive toxicity and endocrine system disruption to fish, it is crucial to identify environmental chemicals with anti-androgenic potential and to develop sensitive detection methods to assess anti-androgenic responses in fish. Although many evaluation systems have been established for detecting estrogenic activity of chemicals, few methods have been developed to identify anti-androgenic effects using fish species, such as three-spined stickleback (*Gasterosteus aculeatus*), Japanese medaka, and *spiggin-gfp* medaka. However, these testing methods require longer exposure durations and specific maintenance systems.

The susceptibility of organisms to chemical exposure is high during the earlier developmental stage, and chemical exposures during this period can cause irreversible outcomes such as malformation. Extensive studies have investigated the developmental effects of chemical exposure, but their connection to endocrine-disrupting effects remains unclear. Zebrafish, as a cost-effective and high fertility animal model, has been widely used in various research fields, including drug screening, gene function analyzing, developmental toxicity measuring, and endocrine-disrupting study. In recent years, molecular docking simulations have become essential in structure-based computational studies aimed at enhancing our understanding of receptor-ligand interactions at the atomic level. In this study, we used *in vivo* and *in silico* methods to develop a simple and rapid

evaluation system to test anti-androgenic effects, which has been rarely reported so far. This study aimed to clarify the anti-androgenic effects of various environmental chemicals using the constructed evaluation system. Furthermore, we aimed to clarify the developmental toxicity of each environmental chemical and to evaluate the relationship between endocrine disrupting effects and developmental toxicity.

Chapter I established zebrafish-based *in vivo* and *in silico* assay systems to evaluate the anti-androgenic potential of environmental chemicals. Zebrafish embryos were exposed to 17α-methyltestosterone (TES) alone or in combination with the anti-androgen flutamide (FLU), as well as various pesticides known for their anti-androgenic activities, such as *p,p′*-DDE (DDE), vinclozolin (VIN), linuron (LIN), and fenitrothion (FEN). In order to explore the potential correlation between anti-androgenic potency and developmental toxicity, this chapter additionally conducted morphological assessments.

The expression of sulfotransferase family 2st3 (*sult2st3*), was measured as an indicator of anti-androgenic effects. The expression of *sult2st3* mRNA was significantly induced by TES in the later developmental stages of embryos. However, the TES-induced expression of *sult2st3* was inhibited by anti-androgen FLU in a concentration-dependent manner with IC_{50} of 5.7 μM, suggesting that the androgen receptor (AR) plays a role in *sult2st3* induction. Similarly, DDE, VIN, and LIN repressed the TES-induced expression of *sult2st3* with IC_{50} of 0.35, 3.90, and 52.00 μM, respectively. At the highest concentration tested (100 μM), FEN also suppressed *sult2st3* expression almost completely, although its IC_{50} could not be calculated. Notably, DDE and LIN did not inhibit *sult2st3* induction due to higher concentrations of TES; instead, they potentiated TES-induced *sult2st3* expression. All tested pesticides affected the swim bladder inflation, especially FLU, VIN, LIN, and FEN impaired swim bladder inflation in a concentration-dependent manner. FLU, LIN, and FEN caused significant mortality at 30 uM, 300 uM, and 100 uM, respectively. LIN and FEN, which had relatively low anti-

androgenic potentials in terms of *sult2st3* inhibition, induced broader toxicities in zebrafish embryos. Thus, the relationship between developmental toxicities and anti-androgenic potency was unclear. Additionally, an *in silico* docking simulation showed that all five chemicals interact with the zebrafish AR at relatively low interaction energies and with Arg702 as a key amino acid in ligand binding, whereas several chemicals classified into other groups (e.g., potassium permanganate, 4-hydroxytamoxifen, and 20-hydroxyecdysone) have higher interaction energies. This indicates that anti-androgenic compounds exhibit a higher stability in bonding with zfAR compared to compounds not classified into anti-androgens.

The *in vivo* and *in vitro* anti-androgenic and anti-estrogenic effects of bisphenol A (BPA) have been reported. Still, there is limited research on its analogs about these aspects. Therefore, Chapter II aimed to measure the anti-androgenic potency of BPA and its various analogs applied the established method in Chapter I, and to test their anti-estrogenic potentials both *in vivo* and *in silico*. To better understand the involvement of estrogen receptor (ER) signaling in the developmental toxicity of BPA and its analogs, this chapter also performed morphological assessments of cardiovascular toxicity, such as pericardial edema and blood flow reduction.

For gene expression analysis, zebrafish embryos were exposed to TES or 17β-estradiol (E2) alone or in combination with BPA or each of its analogs, such as bisphenol AF (BPAF), bisphenol E (BPE), bisphenol F (BPF), bisphenol B (BPB), bisphenol C2 (BP C2), 2,2′-bisphenol F (2,2′-BPF), 4,4′-(1,3-dimethylbutylidene)diphenol (Bis-MP), bisphenol Z (BPZ), and bisphenol S (BPS), at 72 h postfertilization. After 24 h of exposure, all samples were collected to measure the mRNA expression levels of *sult2st3* and *CYP19A1b*, which were used to assess the anti-androgenic and estrogenic potential of the tested compounds, respectively. To better understand the ligand binding affinity, we analyzed the binding mode of bisphenols to the zebrafish AR and estrogen receptor subtypes (ERα,

ERβ1, and ERβ2). For morphological assessment, embryos were exposed to BPA or its analogs in the presence or absence of ER antagonist fulvestrant (ICI) at 72 hpf and were observed at 96 hpf.

BPAF, BPE, BPA, BPF, and BPB inhibited the expression of TES-induced *sult2st3* with IC_{50} values of 0.53, 3.7, 4.7, 12, and 87 μM, respectively. BP C2, 2,2′-BPF, and Bis-MP showed an inhibitory effect on TES-induced *sult2st3* at the higher tested concentrations. However, BPZ and BPS did not exhibit inhibitory effects on TES-induced *sult2st3*. These results indicate that the anti-androgenic effect of BPA and its analogs follows this order: BPAF > BPE > BPA > BPF > BPB > BP C2 > 2,2′-BPF > Bis-MP >> BPZ ≈ BPS. In AR ligand binding domain, BPA formed a hydrogen bond with Met695, while most of analogs hydrogen-bonded to Asn655 and/or Gln661, indicating that these amino acid residues are essential for exhibiting anti-androgenic activity of bisphenols. Furthermore, BPAF, BPA, BPF, BPB, BP C2, and Bis-MP showed inhibitory effects on E2-induced *CYP19A1b* expression in a concentration-independent manner, indicating their anti-estrogenic effects. Compared to our previous study, the binding mode of BPA and its analogs differed between their antagonistic and agonistic effects on ER subtypes. Specifically, ERβ2 exhibited completely distinct binding modes for bisphenols in the agonistic and antagonistic modes, suggesting the potential role of ERβ2 in distinguishing agonistic and antagonistic activities of bisphenols. BP C2, Bis-MP, and BPAF showed more potent cardiovascular toxicity, as their lowest observed effect concentrations are much lower than those of BPA, BPE, and BPF. The incidence of pericardial edema and blood flow reduction induced by BP C2, Bis-MP, and BPAF was large/completely reduced by ICI, whereas this effect was not observed with BPA, BPE, and BPF. This suggests that ER signaling may not mediate the cardiovascular toxicity induced by BPA, BPE, or BPF.

In summary, the present study provided the faster and simpler *in vivo* methods for assessing anti-androgenic potentials of a wider range of environmental chemicals using zebrafish embryos. The majority of tested bisphenols exhibited both anti-androgenic and anti-estrogenic effects, while BPZ

and BPS did not demonstrate either. No correlation was observed between the concentration-dependent effects of anti-androgenic or anti-estrogenic activities and their cardiovascular toxicity. Some BPA alternatives, such as BP C2, Bis-MP, and BPAF, showed stronger cardiovascular toxicity than BPA, BPE, and BPF. The cardiovascular toxicity caused by BPA, BPE, and BPF may not be mediated by ER signaling, but further investigations are needed to confirm the (non)involvement of ER in cardiovascular toxicity induced by these bisphenols. Based on our findings, utilizing zebrafish-based *in vivo* and *in silico* assessments appears to be a promising approach for evaluating the anti-androgenic or anti-estrogenic potentials of environmental chemicals. Careful consideration should be given to the toxicities of alternative itself when selecting BPA replacement.

要約

第二次世界大戦以降、多種多様な化学物質が生産・使用され人類に利便性をもたらしてきた。一方、生産・使用された化学物質が環境中に放出され、中には極微量で生物の内分泌系を撹乱する作用を示すいわゆる内分泌撹乱物質（環境ホルモン）が含まれていることも明らかにされてきた。とくに、あらゆる環境化学物質の到達点である水圏において、内分泌撹乱物質の生態系に対する影響が懸念されたため、こうした視点の研究がこれまで数多く実施されてきた。魚類を用いた研究では、環境化学物質がエストロゲン作用や抗アンドロゲン作用を示し、メス化と関連することが報告されている。したがって、多様な化学物質についてエストロゲン作用や抗アンドロゲン作用を魚類で評価することは重要である。これまでエストロゲン作用の評価系については多くの報告例があるものの、抗アンドロゲン作用の評価系については報告例が少なく、また評価にかかる時間やコストなどの面で課題もあった。

一般に化学物質に対する感受性は発達期で高く、その時期における曝露は奇形等の不可逆的かつ重大な影響を引き起こす。これまでに化学物質の発達期での影響を調べた研究は多いが、内分泌撹乱作用との関連性については不明な点が多い。

本研究では、環境毒性学研究ですでに重要な地位を築いているゼブラフィッシュをモデルとして、インビボ試験およびインシリコ手法を用いて、これまでに報告例の少ない抗アンドロゲン作用の簡便迅速な評価系を構築すること、ならびに構築した評価系を用いて多様な環境化学物質の抗アンドロゲン作用を明らかにすることを目的とした。さらに、各環境化学物質の発生毒性を明らかにするとともに、抗アンドロゲン作用と発生毒性の関連性について評価することも目的とした。

第 I 章では、抗アンドロゲン作用の評価系の構築について検討した。まずインビボ試験では、アンドロゲン活性のマーカー遺伝子として知られる sulfotransferase 2st3（*sult2st3*）を指標として、テストステロン（TES）誘導性の *sult2st3* 発現に対する化学物質の抑制能を評価した。このため、受精後 72 時間のゼブラフィッシュ胚にメチルテストステロンならびにこれまで抗アンドロゲン作用が報告されているフルタミド（FUL）と 4 種の農薬（*p,p'*-DDE（DDE）、ビンクロゾリン（VIN）、リニュロン（LIN）、フェニトロチオン（FEN））をそれぞれ共曝露した。受精後96時間で発生毒性を評価した後、曝露胚を採材した。採材した曝露胚は、全 RNA 抽出をした後、cDNA 合成を行い、リアルタイム PCR 法で *sult2st3* の発現量を測定した。曝露試験の結果、TES 誘導性の *sult2st3* 発現量は抗アンドロゲン剤 FLU によって濃度依存的に抑制され、その用量効果（IC_{50}）は 5.7 μM であった。したがって、TES による *sult2st3* 発現誘導にはアンドロゲン受容体（AR）が関与して

いると考えられた。同様に、DDE、VIN、LIN についても、それぞれ TES 誘導性の *sult2st3* 発現量は濃度依存的に抑制され、IC_{50} はそれぞれ、0.35μM、3.9μM、52μM であった。FEN については、本曝露試験の最高濃度である 100μM でのみ、TES 誘導性の *sult2st3* 発現の抑制が認められた。また、TES 誘導性の *sult2st3* 発現の抑制に関する用量効果が相対的に低かった FEN と LIN において、高濃度側で循環障害や浮袋の膨張不全など様々な発生毒性が認められた。これらの結果より、発生毒性と抗アンドロゲン作用の間に明瞭な相関性は認められなかった。

次いで、インシリコ解析では、ヒト AR と水酸化フルタミド（hydroxyflutamide）の結晶構造をテンプレートとして、ホモロジーモデリングによりゼブラフィッシュ AR（zfAR）の 3 次元構造を構築した。構築した zfAR と、上記のインビボ試験で抗アンドロゲン作用を評価した化合物についてドッキングシミュレーションを行い、リガンド結合に重要な役割を果たしているアミノ酸を推定するとともに、相互作用エネルギーを算出した。インシリコ解析の結果、FUL、DDE、VIN、LIN、FEN の 5 化合物は、いずれも zfAR のリガンド結合ポケットに位置する Arg702 と水素結合を形成し、その相互作用エネルギーは抗アンドロゲン作用をもたない他の化合物群と比べて相対的に低い値をもつことが示された。以上より、インビボ試験で抗アンドロゲン作用を示した化合物は、他の化合物群と比べて zfAR とより安定的に結合することが示唆された。

第 II 章では、第 I 章で構築した抗アンドロゲン作用のインビボ・インシリコ評価系を用いて、ビスフェノール A（BPA）とその関連化合物（ビスフェノール類）の抗アンドロゲン作用を評価した。加えて、エストロゲン受容体（ER）の標的遺伝子である *CYP19A1b* を指標として、17β-エストラジオール（E2）誘導性の *CYP19A1b* 発現に対する各ビスフェノール類の抑制能（抗エストロゲン作用）を評価した。このためインビボ試験では、受精後 72 時間のゼブラフィッシュ胚に TES または E2 と、各ビスフェノール類をそれぞれ共曝露した。いずれも受精後 96 時間で曝露胚を採材し、全 RNA 抽出をした後、cDNA 合成を行い、リアルタイム PCR 法で *sult2st3* または *CYP19A1b* の発現量を測定した。さらに、BPA および一部のビスフェノール類（BPE、BPF、BP C2、Bis-MP、BPAF）については、同様に曝露試験を行い、心臓周囲浮腫や体幹血流の低下を評価した。また、ER 拮抗薬であるフルベストラント（ICI）との共曝露試験を行い、ビスフェノール類の発生毒性に対する ER の関与を検討した。

抗アンドロゲン作用に関する曝露試験の結果、TES 誘導性の *sult2st3* 発現量は多くのビスフェノール類によって濃度依存的に抑制され、その用量効果（IC_{50}）は BPAF（0.53μM）、BPE（3.7μM）、BPA（4.7μM）、BPF（12μM）、および BPB（87 μM）の順であった。また、BP C2、2,2′-BPF、および Bis-MP は、試験した最高濃度でのみ TES 誘導性の *sult2st3* 発現を抑制した。一方、BPZ および BPS は TES 誘導性の *sult2st3* 発現を抑制

しなかった。次いで、インシリコ解析では、BPA は zfAR のリガンド結合ポケットに位置する Met695 と水素結合を形成し、その他のビスフェノール類の多くは Asn655 もしくは Gln661 と水素結合を形成した。したがって、これらアミノ酸残基がビスフェノール類の抗アンドロゲン作用で重要な役割を担うと推察された。

抗エストロゲン作用に関する曝露試験の結果、E2 誘導性の *CYP19A1b* 発現は、試験した高濃度の BPAF、BPA、BPF、BPB、BP C2、および Bis-MP によって抑制されたものの、明瞭な濃度依存性は認められなかった。したがって、これらビスフェノール類は、用量効果は低いものの抗エストロゲン作用を有することが示唆された。次いで、インシリコ解析では、多くのビスフェノール類は各 ER サブタイプ（zfERα、zfERβ1、zfERβ2）のリガンド結合ポケットに位置するアミノ酸残基と水素結合を形成した。さらに、本研究で明らかにした ER アンタゴニスト作用に関する結合モードは、当研究グループのこれまでの研究で明らかにした ER アゴニスト作用に関する結合モードと異なることが示された。とくに、ERβ2 ではアゴニスト作用とアンタゴニスト作用でまったく異なる結合モードを示したことから、ERβ2 がビスフェノールのアゴニスト作用とアンタゴニスト作用を区別する重要な役割をもつことが示唆された。

ビスフェノール類の曝露胚における心血管毒性の評価では、試験したいずれのビスフェノール類（BPA、BPE、BPF、BP C2、Bis-MP、BPAF）についても、心臓周囲浮腫や体

幹血流の低下が認められた。その用量効果は、BP C2、Bis-MP、および BPAF で高く、逆に BPA、BPE、および BPF では低かった。また、BP C2、Bis-MP、および BPAF で誘発された心臓周囲浮腫および体幹血流の低下は ICI によって大幅に改善したが、同様の改善効果は BPA、BPE、および BPF 誘発性の心血管毒性では観察されなかった。したがって、BPA、BPE、BPF 誘発性の心血管毒性は ER シグナル介在性ではないと考えられた。

以上の結果より、多くのビスフェノール類は、抗アンドロゲン作用と抗エストロゲン作用の両方を有することが明らかとなった。一方、試験したビスフェノール類では、抗アンドロゲン作用や抗エストロゲン作用の用量効果と心血管毒性の用量効果の間に相関関係は認められなかったことから、ビスフェノール類誘発性の心血管毒性は ER や AR 介在性ではないと推察された。一方で、BPA よりも抗アンドロゲン作用、抗エストロゲン作用、心血管毒性のいずれも高いビスフェノール類が複数あることが明らかとなったことから、構造的に類似の代替物質を利用する際にはそれらの毒性を明らかにする必要があると考えられた。

References

Akan, J.C., Battah, N., Waziri, M., Mahmud, M.M., 2015. Organochlorine, organophosphorus and pyrethroid pesticides residues in water and sediment samples from River Benue in Vinikilang, Yola, Adamawa State, Nigeria using Gas Chromatography-Mass Spectrometry equipped with Electron Capture Detector ". Am. J. Environ. Prot. 3, 164–173. https://doi.org/10.12691/env-3-5-2

Alnouti, Y., Klaassen, C.D., 2008. Regulation of sulfotransferase enzymes by prototypical microsomal enzyme inducers in mice. J. Pharmacol. Exp. Ther. 324, 612–621. https://doi.org/10.1124/jpet.107.129650

Amutova, F., Delannoy, M., Baubekova, A., Konuspayeva, G., Jurjanz, S., 2021. Transfer of persistent organic pollutants in food of animal origin – Meta-analysis of published data. Chemosphere. https://doi.org/10.1016/j.chemosphere.2020.128351

Ankley, G.T., Jensen, K.M., Durhan, E.J., Makynen, E.A., Butterworth, B.C., Kahl, M.D., Villeneuve, D.L., Linnum, A., Gray, L.E., Cardon, M., Wilson, V.S., 2005. Effects of two fungicides with multiple modes of action on reproductive endocrine function in the fathead minnow (Pimephales promelas). Toxicol. Sci. 86, 300–308. https://doi.org/10.1093/toxsci/kfi202

Araki, N., Ohno, K., Nakai, M., Takeyoshi, M., Iida, M., 2005. Screening for androgen receptor activities in 253 industrial chemicals by in vitro reporter gene assays using AR-EcoScreen™ cells. Toxicol. Vitr. 19, 831–842. https://doi.org/10.1016/j.tiv.2005.04.009

Aullón, G., Bellamy, D., Guy Orpen, A., Brammer, L., Bruton, E.A., 1998. Metal-bound chlorine often accepts hydrogen bonds. Chem. Commun 653–654. https://doi.org/DOI https://doi.org/10.1039/A709014E

Braun, J.M., Kalkbrenner, A.E., Calafat, A.M., Yolton, K., Ye, X., Dietrich, K.N., Lanphear, B.P., 2011. Impact of early-life bisphenol A exposure on behavior and executive function in children. Pediatrics 128, 873–882. https://doi.org/10.1542/peds.2011-1335

Cao, X.L., Perez-Locas, C., Robichaud, A., Clement, G., Popovic, S., Dufresne, G., Dabeka, R.W., 2015. Levels and temporal trend of bisphenol A in composite food samples from Canadian Total Diet Study 2008–2012. Food Addit. Contam. - Part A Chem. Anal. Control. Expo. Risk Assess. 32, 2154–2160. https://doi.org/10.1080/19440049.2015.1088663

Cariati, F., D'Uonno, N., Borrillo, F., Iervolino, S., Galdiero, G., Tomaiuolo, R., 2019. "Bisphenol a: an emerging threat to male fertility." Reprod. Biol. Endocrinol. 17, 6. https://doi.org/10.1186/s12958-018-0447-6

Caux, P.Y., Kent, R.A., Fan, G.T., Grande, C., 1998. Canadian water quality guidelines for linuron. Environ. Toxicol. Water Qual. 13, 1–41. https://doi.org/10.1002/(SICI)1098-2256(1998)13:1<1::AID-TOX1>3.0.CO;2-B

Chen, D., Kannan, K., Tan, H., Zheng, Z., Feng, Y.L., Wu, Y., Widelka, M., 2016. Bisphenol Analogues Other Than BPA: Environmental Occurrence, Human Exposure, and Toxicity - A Review. Environ. Sci. Technol. 50, 5438–5453. https://doi.org/10.1021/acs.est.5b05387

Chen, X., Hirano, M., Ishibashi, H., Lee, J.S., Kawai, Y.K., Kubota, A., 2023. Efficient in vivo and in silico assessments of antiandrogenic potential in zebrafish. Comp. Biochem. Physiol. Part C Toxicol. Pharmacol. 264, 109513. https://doi.org/10.1016/j.cbpc.2022.109513

Colborn, T., Vom Saal, F.S., Soto, A.M., 1993. Developmental effects of endocrine-disrupting chemicals in wildlife and humans. Environ. Health Perspect. 101, 378–384. https://doi.org/10.1289/ehp.93101378

Conroy-Ben, O., Garcia, I., Teske, S.S., 2018. In silico binding of 4,4'-bisphenols predicts in vitro estrogenic and antiandrogenic activity. Environ. Toxicol. 33, 569–578. https://doi.org/10.1002/tox.22539

Deceuninck, Y., Bichon, E., Marchand, P., Boquien, C.Y., Legrand, A., Boscher, C., Antignac, J.P., Le Bizec, B., 2015. Determination of bisphenol A and related substitutes/analogues in human breast milk using gas chromatography-tandem mass spectrometry. Anal. Bioanal. Chem. 407, 2485–2497. https://doi.org/10.1007/s00216-015-8469-9

Delfosse, V., Grimaldi, M., Pons, J.L., Boulahtouf, A., Le Maire, A., Cavailles, V., Labesse, G., Bourguet, W., Balaguer, P., 2012. Structural and mechanistic insights into bisphenols action provide guidelines for risk assessment and discovery of bisphenol A substitutes. Proc. Natl. Acad. Sci. U. S. A. 109, 14930–14935. https://doi.org/10.1073/pnas.1203574109

Di Toro, D.M., McGrath, J.A., Stubblefield, W.A., 2007. Predicting the toxicity of neat and weathered crude oil: Toxic potential and the toxicity of saturated mixtures. Environ. Toxicol. Chem. 26, 24–36. https://doi.org/10.1897/06174R.1

Dishaw, L. V., Hunter, D.L., Padnos, B., Padilla, S., Stapleton, H.M., 2014. Developmental exposure to organophosphate flame retardants elicits overt toxicity and alters behavior in early life stage zebrafish (danio rerio). Toxicol. Sci. 142, 445–454. https://doi.org/10.1093/toxsci/kfu194

Duanmu, Z., Locke, D., Smigelski, J., Wu, W., Dahn, M.S., Falany, C.N., Kocarek, T.A., Runge-Morris, M., 2002. Effects of dexamethasone on aryl (SULT1A1)- and hydroxysteroid (SULT2A1)-sulfotransferase gene expression in primary cultured human hepatocytes. Drug Metab. Dispos. 30, 997–1004. https://doi.org/10.1124/dmd.30.9.997

EFSA, 2015. Scientific Opinion on the risks to public health related to the presence of bisphenol A (BPA) in foodstuffs. Eur. Food Saf. Auth. 13, 3978. https://doi.org/https://doi.org/10.2903/j.efsa.2015.3978

El-Shahat, M.F., Al-Nawayseh, K.M., Jiries, A.G., Alnasir, F.M., 2003. Pesticides and Heavy Metal Distribution in Southern Dead Sea Basin. Bull. Environ. Contam. Toxicol. 71, 1230–1238. https://doi.org/10.1007/s00128-003-8789-x

Fent, K., Siegenthaler, P.F., Schmid, A.A., 2018. Transcriptional effects of androstenedione and 17A-hydroxyprogesterone in zebrafish embryos. Aquat. Toxicol. 202, 1–5. https://doi.org/10.1016/j.aquatox.2018.06.012

Fetter, E., Smetanová, S., Baldauf, L., Lidzba, A., Altenburger, R., Schüttler, A., Scholz, S., 2015. Identification and Characterization of Androgen-Responsive Genes in Zebrafish Embryos. Environ. Sci. Technol. 49, 11789–11798. https://doi.org/10.1021/acs.est.5b01034

Freyberger, A., Weimer, M., Tran, H.S., Ahr, H.J., 2010. Assessment of a recombinant androgen receptor binding assay: Initial steps towards validation. Reprod. Toxicol. 30, 2–8. https://doi.org/10.1016/J.REPROTOX.2009.10.001

Fromme, H., Küchler, T., Otto, T., Pilz, K., Müller, J., Wenzel, A., 2002. Occurrence of phthalates and bisphenol A and F in the environment. Water Res. https://doi.org/10.1016/S0043-1354(01)00367-0

Gibson, R., Smith, M.D., Spary, C.J., Tyler, C.R., Hill, E.M., 2005. Mixtures of estrogenic contaminants in bile of fish exposed to wastewater treatment works effluents. Environ. Sci. Technol. 39, 2461–2471. https://doi.org/10.1021/es048892g

Gilbertson, M., Kubiak, T., Ludwig, J., Fox, G., 1991. Great lakes embryo mortality, edema, and deformities syndrome (glemeds) in colonial fish-eating birds: Similarity to chick-edema disease. J. Toxicol. Environ. Health 33, 455–520. https://doi.org/10.1080/15287399109531538

Goldstone, J. V., McArthur, A.G., Kubota, A., Zanette, J., Parente, T., Jönsson, M.E., Nelson, D.R., Stegeman, J.J., 2010. Identification and developmental expression of the full complement of Cytochrome P450 genes in Zebrafish. BMC Genomics 11. https://doi.org/10.1186/1471-2164-11-643

Halgren, T.A., 1996. Merck Molecular Force Field. J. Comput. Chem. 17, 490–519. https://doi.org/https://doi.org/10.1002/(SICI)1096-987X(199604)17:5/6<490::AID-JCC1>3.0.CO;2-P

Harris, E.P., Allardice, H.A., Schenk, A.K., Rissman, E.F., 2018. Effects of maternal or paternal bisphenol A exposure on offspring behavior. Horm. Behav. 101, 68–76. https://doi.org/10.1016/j.yhbeh.2017.09.017

Herve, M., 2022. RVAideMemoire: Testing and Plotting Procedures for Biostatistics. https://doi.org/https://cran.r-project.org/package=RVAideMemoire

Hill, E.M., Evans, K.L., Horwood, J., Rostkowski, P., Oladapo, F.O., Gibson, R., Shears, J.A., Tyler, C.R., 2010. Profiles and some initial identifications of (anti)androgenic compounds in fish exposed to wastewater treatment works effluents. Environ. Sci. Technol. 44, 1137–1143. https://doi.org/10.1021/es901837n

Hossain, M.S., Chowdhury, M.A.Z., Pramanik, M.K., Rahman, M.A., Fakhruddin, A.N.M., Alam, M.K., 2015. Determination of selected pesticides in water samples adjacent to agricultural fields and removal of organophosphorus insecticide chlorpyrifos using soil bacterial isolates. Appl. Water Sci. 5, 171–179. https://doi.org/10.1007/s13201-014-0178-6

Hossain, M.S., Larsson, A., Scherbak, N., Olsson, P.E., Orban, L., 2008. Zebrafish androgen receptor: Isolation, molecular, and biochemical characterization. Biol. Reprod. 78, 361–369. https://doi.org/10.1095/biolreprod.107.062018

Ikeuchi, T., Todo, T., Kobayashi, T., Nagahama, Y., 2001. Two subtypes of androgen and progestogen receptors in fish testes. Comp. Biochem. Physiol. - B Biochem. Mol. Biol. 129, 449–455. https://doi.org/10.1016/S1096-4959(01)00375-X

Ikezuki, Y., Tsutsumi, O., Takai, Y., Kamei, Y., Taketani, Y., 2002. Determination of bisphenol A concentrations in human biological fluids reveals significant early prenatal exposure. Hum. Reprod. 17, 2839–2841. https://doi.org/10.1093/humrep/17.11.2839

Jarque, S., Ibarra, J., Rubio-Brotons, M., García-Fernández, J., Terriente, J., 2019. Multiplex analysis platform for endocrine disruption prediction using zebrafish. Int. J. Mol. Sci. 20, 1739. https://doi.org/10.3390/ijms20071739

Jemal, T., Astatke, H., Terfe, A., Mekonen, S., 2022. Effect of Conventional and Household Water Treatment Technologies on Pesticide Residues in Drinking Water , Southwestern , Ethiopia 1–18. https://doi.org/https://doi.org/10.21203/rs.3.rs-1372978/v1

Jie, S., Jianchao, L., Guanghua, L., Xiaoxiang, D., 2018. A Review of the Occurrence, Toxicology and Ecological Risk Assessment of Bisphenol S and F in Aquatic Environment. Asian J. Ecotoxicol. 5, 37–48. https://doi.org/doi: 10.7524/AJE.1673-5897.20171009001

Jin, H., Zhu, L., 2016. Occurrence and partitioning of bisphenol analogues in water and sediment from Liaohe River Basin and Taihu Lake, China. Water Res. 103, 343–351. https://doi.org/10.1016/j.watres.2016.07.059

Jobling, S., Burn, R.W., Thorpe, K., Williams, R., Tyler, C., 2009. Statistical modeling suggests that antiandrogens in effluents from wastewater treatment works contribute to widespread sexual disruption in fish living in english rivers. Environ. Health Perspect. 117, 797–802. https://doi.org/10.1289/ehp.0800197

Jolly, C., Katsiadaki, I., Morris, S., Le Belle, N., Dufour, S., Mayer, I., Pottinger, T.G., Scott, A.P., 2009. Detection of the anti-androgenic effect of endocrine disrupting environmental

contaminants using in vivo and in vitro assays in the three-spined stickleback. Aquat. Toxicol. 92, 228–239. https://doi.org/10.1016/j.aquatox.2009.02.006

Jørgensen, A., Andersen, O., Bjerregaard, P., Rasmussen, L.J., 2007. Identification and characterisation of an androgen receptor from zebrafish Danio rerio. Comp. Biochem. Physiol. - C Toxicol. Pharmacol. 146, 561–568. https://doi.org/10.1016/j.cbpc.2007.07.002

Kameya, T., Saito, M., Kondo, T., Toriumi, W., Fujie, K., Matsushita, T., Takanashi, H., 2012. Detection of Fenitrothion and its Degradation Product 3-Methyl-4-nitrophenol in Water Environment. J. Water Environ. Technol. 10, 427–436. https://doi.org/10.2965/jwet.2012.427

Kelce, W.R., Monosson, E., Gamcsik, M.P., Laws, S.C., Gray, L.E., 1994. Environmental Hormone Disruptors: Evidence That Vinclozolin Developmental Toxicity Is Mediated by Antiandrogenic Metabolites. Toxicol. Appl. Pharmacol. 126, 276–285. https://doi.org/10.1006/taap.1994.1117

Kitamura, S., Suzuki, T., Sanoh, S., Kohta, R., Jinno, N., Sugihara, K., Yoshihara, S., Fujimoto, N., Watanabe, H., Ohta, S., 2005. Comparative study of the endocrine-disrupting activity of bisphenol A and 19 related compounds. Toxicol. Sci. 84, 249–259. https://doi.org/10.1093/toxsci/kfi074

Kojima, H., Katsura, E., Takeuchi, S., Niiyama, K., Kobayashi, K., 2004. Screening for estrogen and androgen receptor activities in 200 pesticides by in vitro reporter gene assays using Chinese hamster ovary cells. Environ. Health Perspect. 112, 524–531. https://doi.org/10.1289/ehp.6649

Kojima, H., Takeuchi, S., Sanoh, S., Okuda, K., Kitamura, S., Uramaru, N., Sugihara, K., Yoshinari, K., 2019. Profiling of bisphenol A and eight its analogues on transcriptional activity via human nuclear receptors. Toxicology 413, 48–55. https://doi.org/10.1016/j.tox.2018.12.001

Koninckx, P.P., 1999. The physiopathology of endometriosis: Pollution and dioxin. Gynecol. Obstet. Invest. 47, 47–50. https://doi.org/10.1159/000052859

Kretschmer, X.C., Baldwin, W.S., 2005. CAR and PXR: Xenosensors of endocrine disrupters? Chem. Biol. Interact. 155, 111–128. https://doi.org/10.1016/j.cbi.2005.06.003

Kubota, A., Hirano, M., Yoshinouchi, Y., Chen, X., Nakamura, M., Wakayama, Y., Lee, J.S., Nakata, H., Iwata, H., Kawai, Y.K., 2023. In vivo and in silico assessments of estrogenic potencies of bisphenol A and its analogs in zebrafish (Danio rerio): Validity of in silico approaches to predict in vivo effects. Comp. Biochem. Physiol. Part C Toxicol. Pharmacol. 269, 109619. https://doi.org/10.1016/j.cbpc.2023.109619

Kubota, A., Kawai, Y.K., Yamashita, N., Lee, J.S., Kondoh, D., Zhang, S., Nishi, Y., Suzuki, K., Kitazawa, T., Teraoka, H., 2019. Transcriptional profiling of cytochrome P450 genes in the liver of adult zebrafish, Danio rerio. J. Toxicol. Sci. 44, 347–356. https://doi.org/10.2131/jts.44.347

Kundakovic, M., Gudsnuk, K., Franks, B., Madrid, J., Miller, R.L., Perera, F.P., Champagne, F.A., 2013. Sex-specific epigenetic disruption and behavioral changes following low-dose in utero bisphenol a exposure. Proc. Natl. Acad. Sci. U. S. A. 110, 9956–9961. https://doi.org/10.1073/pnas.1214056110

Labute, P., 2008. The Generalized Born/Volume Integral Implicit Solvent Model: Estimation of the Free Energy of Hydration Using London Dispersion Instead of Atomic Surface Area. J. Comput. Chem. 29, 1693–1698. https://doi.org/10.1002/jcc

Labute, P., Williams, C., 2015. Application of Hückel Theory to Pharmacophore Discovery. CICSJ Bull. 33, 33. https://doi.org/https://doi.org/10.11546/cicsj.33.33

Lambright, C., Ostby, J., Bobseine, K., Wilson, V., Hotchkiss, A.K., Mann, P.C., Gray, L.E., 2000. Cellular and molecular mechanisms of action of linuron: An antiandrogenic herbicide that

produces reproductive malformations in male rats. Toxicol. Sci. 56, 389–399. https://doi.org/10.1093/toxsci/56.2.389

Lange, A., Sebire, M., Rostkowski, P., Mizutani, T., Miyagawa, S., Iguchi, T., Hill, E.M., Tyler, C.R., 2015. Environmental chemicals active as human antiandrogens do not activate a stickleback androgen receptor but enhance a feminising effect of oestrogen in roach. Aquat. Toxicol. 168, 48–59. https://doi.org/10.1016/j.aquatox.2015.09.014

Lee, H.J., Chattopadhyay, S., Gong, E.-Y., Ahn, R.S., Lee, K., 2003. Antiandrogenic effects of bisphenol A and nonylphenol on the function of androgen receptor. Toxicol. Sci. 75, 40–46.

Lee, J.S., Morita, Y., Kawai, Y.K., Covaci, A., Kubota, A., 2020. Developmental circulatory failure caused by metabolites of organophosphorus flame retardants in zebrafish, Danio rerio. Chemosphere 246. https://doi.org/10.1016/j.chemosphere.2019.125738

Li, J., Li, N., Ma, M., Giesy, J.P., Wang, Z., 2008. In vitro profiling of the endocrine disrupting potency of organochlorine pesticides. Toxicol. Lett. 183, 65–71. https://doi.org/10.1016/j.toxlet.2008.10.002

Liao, C., Liu, F., Alomirah, H., Loi, V.D., Mohd, M.A., Moon, H.-B., Nakata, H., Kannan, K., 2012a. Bisphenol S in Urine from the United States and Seven Asian Countries: Occurrence and Human Exposures. Environ. Sci. Technol. 46, 6860–6866. https://doi.org/10.1021/es301334j

Liao, C., Liu, F., Guo, Y., Moon, H.-B., Nakata, H., Wu, Q., Kannan, K., 2012b. Occurrence of Eight Bisphenol Analogues in Indoor Dust from the United States and Several Asian Countries: Implications for Human Exposure. Environ. Sci. Technol. 46, 9138–9145. https://doi.org/10.1021/es302004w

Liao, C., Liu, F., Moon, H.B., Yamashita, N., Yun, S., Kannan, K., 2012c. Bisphenol analogues in sediments from industrialized areas in the United States, Japan, and Korea: Spatial and

temporal distributions. Environ. Sci. Technol. 46, 11558–11565. https://doi.org/10.1021/es303191g

Livak, K.J., Schmittgen, T.D., 2001. Analysis of relative gene expression data using real-time quantitative PCR and the 2-ΔΔCT method. Methods 25, 402–408. https://doi.org/10.1006/meth.2001.1262

Löser, R., Seibel, K., Roos, W., Eppenberger, U., 1985. In vivo and in vitro antiestrogenic action of 3-hydroxytamoxifen, tamoxifen and 4-hydroxytamoxifen. Eur. J. Cancer Clin. Oncol. 21, 985–990. https://doi.org/10.1016/0277-5379(85)90119-1

Martinovic´, D., Blake, L.S., Durhan, E.J., Greene, K.J., Kahl, M.D., Jensen, K.M., Makynen, E.A., Villeneuve, D.L., Ankley, G.T., 2008. Reproductive toxicity of vinclozolin in the fathead minnow: Confirming an anti-androgenic mode of action. Environ. Toxicol. Chem. 27, 478–488. https://doi.org/https://doi.org/10.1897/07-206R.1

McIntyre, B.S., Barlow, N.J., Foster, P.M.D., 2001. Androgen-mediated development in male rat offspring exposed to flutamide in utero: Permanence and correlation of early postnatal changes in anogenital distance and nipple retention with malformations in androgen-dependent tissues. Toxicol. Sci. 62, 236–249. https://doi.org/10.1093/toxsci/62.2.236

Meng, X., Su, S., Wei, X., Wang, S., Guo, T., Li, J., Song, H., Wang, M., Wang, Z., 2023. Exposure to bisphenol A alternatives bisphenol AF and fluorene-9-bisphenol induces gonadal injuries in male zebrafish. Ecotoxicol. Environ. Saf. 253, 114634. https://doi.org/10.1016/j.ecoenv.2023.114634

Menuet, A., Pellegrini, E., Anglade, I., Blaise, O., Lauder, V., Kah, O., Pakdel, F., 2002. Molecular characterization of three estrogen receptor forms in zebrafish: Binding characteristics, transactivation properties, and tissue distributions. Biol. Reprod. 66, 1881–1892. https://doi.org/10.1095/biolreprod66.6.1881

Möcklinghoff, S., Rose, R., Carraz, M., Visser, A., Ottmann, C., Brunsveld, L., 2010. Synthesis and Crystal Structure of a Phosphorylated Estrogen Receptor Ligand Binding Domain. ChemBioChem 11, 2251–2254. https://doi.org/10.1002/cbic.201000532

Molina-Molina, J.M., Amaya, E., Grimaldi, M., Sáenz, J.M., Real, M., Fernández, M.F., Balaguer, P., Olea, N., 2013. In vitro study on the agonistic and antagonistic activities of bisphenol-S and other bisphenol-A congeners and derivatives via nuclear receptors. Toxicol. Appl. Pharmacol. 272, 127–136. https://doi.org/10.1016/j.taap.2013.05.015

Moreman, J., Lee, O., Trznadel, M., David, A., Kudoh, T., Tyler, C.R., 2017. Acute Toxicity, Teratogenic, and Estrogenic Effects of Bisphenol A and Its Alternative Replacements Bisphenol S, Bisphenol F, and Bisphenol AF in Zebrafish Embryo-Larvae. Environ. Sci. Technol. 51, 12796–12805. https://doi.org/10.1021/acs.est.7b03283

Mouriec, K., Lareyre, J.J., Tong, S.K., Le Page, Y., Vaillant, C., Pellegrini, E., Pakdel, F., Chung, B.C., Kah, O., Anglade, I., 2009. Early regulation of brain aromatase (cyp19a1b) by estrogen receptors during zebrafish development. Dev. Dyn. 238, 2641–2651. https://doi.org/10.1002/dvdy.22069

Mu, X., Huang, Y., Li, Xuxing, Lei, Y., Teng, M., Li, Xuefeng, Wang, C., Li, Y., 2018. Developmental Effects and Estrogenicity of Bisphenol A Alternatives in a Zebrafish Embryo Model. Environ. Sci. Technol. 52, 3222–3231. https://doi.org/10.1021/acs.est.7b06255

Muñoz-de-Toro, M., Markey, C., Wadia, P.R., Luque, E.H., Rubin, B.S., Sonnenschein, C., Soto, A.M., 2005. Perinatal exposure to Bisphenol A alters peripubertal mammary gland development in mice. Endocrinology 146, 4138–4147. https://doi.org/10.1210/en.2005-0340

Nakamura, A., Takanobu, H., Tamura, I., Yamamuro, M., Iguchi, T., Tatarazako, N., 2014. Verification of responses of Japanese medaka (Oryzias latipes) to anti-androgens, vinclozolin

and flutamide, in short-term assays. J. Appl. Toxicol. 34, 545–553. https://doi.org/10.1002/jat.2934

OECD, 2009. The 21-day androgenised female stickleback endocrine screening assay Defra funded research, in: Test Guidelines for Screening Chemicals with Potential Endocrine Disrupting Activity. https://doi.org/https://www.oecd.org/chemicalsafety/testing/43327146.pdf

Olsson, E., Berg, A.H., Von Hofsten, J., Grahn, B., Hellqvist, A., Larsson, A., Karlsson, J., Modig, C., Borg, B., Thomas, P., 2005. Molecular cloning and characterization of a nuclear androgen receptor activated by 11-ketotestosterone. Reprod. Biol. Endocrinol. 3, 37. https://doi.org/10.1186/1477-7827-3

Orton, F., Rosivatz, E., Scholze, M., Kortenkamp, A., 2011. Widely used pesticides with previously unknown endocrine activity revealed as in Vitro antiandrogens. Environ. Health Perspect. 119, 794–800. https://doi.org/10.1289/ehp.1002895

Park, J.C., Lee, M.C., Yoon, D.S., Han, J., Kim, M., Hwang, U.K., Jung, J.H., Lee, J.S., 2018. Effects of bisphenol A and its analogs bisphenol F and S on life parameters, antioxidant system, and response of defensome in the marine rotifer Brachionus koreanus. Aquat. Toxicol. https://doi.org/10.1016/j.aquatox.2018.03.024

Paulozzi, L.J., 1999. International trends in rates of hypospadias and cryptorchidism. Environ. Health Perspect. 107, 297–302. https://doi.org/10.1289/ehp.99107297

Pelch, K., Wignall, J.A., Goldstone, A.E., Ross, P.K., Blain, R.B., Shapiro, A.J., Holmgren, S.D., Hsieh, J.-H., Svoboda, D., Auerbach, S.S., Parham, F.M., Masten, S.A., Walker, V., Rooney, A., Thayer, K.A., 2019. A scoping review of the health and toxicological activity of bisphenol A (BPA) structural analogues and functional alternatives. Toxicology 424, 152235. https://doi.org/10.1016/j.tox.2019.06.006

Poujol, N., Wurtz, J.M., Tahiri, B., Lumbroso, S., Nicolas, J.C., Moras, D., Sultan, C., 2000. Specific recognition of androgens by their nuclear receptor: A structure-function study. J. Biol. Chem. 275, 24022–24031. https://doi.org/10.1074/jbc.M001999200

Qiu, W., Shao, H., Lei, P., Zheng, C., Qiu, C., Yang, M., Zheng, Y., 2018. Immunotoxicity of bisphenol S and F are similar to that of bisphenol A during zebrafish early development. Chemosphere. https://doi.org/10.1016/j.chemosphere.2017.11.125

Quintaneiro, C., Patrício, D., Novais, S.C., Soares, A.M.V.M., Monteiro, M.S., 2017. Endocrine and physiological effects of linuron and S-metolachlor in zebrafish developing embryos. Sci. Total Environ. 586, 390–400. https://doi.org/10.1016/j.scitotenv.2016.11.153

R Core Team, 2013. R: A Language and Environment for Statistical Computing.

Rochester, J.R., 2013. Bisphenol A and human health: A review of the literature. Reprod. Toxicol. 42, 132–155. https://doi.org/10.1016/j.reprotox.2013.08.008

Rochester, J.R., Bolden, A.L., 2015. Bisphenol S and F: A systematic review and comparison of the hormonal activity of bisphenol a substitutes. Environ. Health Perspect. 123, 643–650. https://doi.org/10.1289/ehp.1408989

Roy, P., Salminen, H., Koskimies, P., Simola, J., Smeds, A., Saukko, P., Huhtaniemi, I.T., 2004. Screening of some anti-androgenic endocrine disruptors using a recombinant cell-based in vitro bioassay. J. Steroid Biochem. Mol. Biol. 88, 157–166. https://doi.org/10.1016/j.jsbmb.2003.11.005

Schmid, S., Willi, R.A., Salgueiro-González, N., Fent, K., 2020. Effects of new generation progestins, including as mixtures and in combination with other classes of steroid hormones, on zebrafish early life stages. Sci. Total Environ. 709. https://doi.org/10.1016/j.scitotenv.2019.136262

Sébillot, A., Damdimopoulou, P., Ogino, Y., Spirhanzlova, P., Miyagawa, S., Du Pasquier, D., Mouatassim, N., Iguchi, T., Lemkine, G.F., Demeneix, B.A., Tindall, A.J., 2014. Rapid fluorescent detection of (anti)androgens with spiggin-gfp medaka. Environ. Sci. Technol. 48, 10919–10928. https://doi.org/10.1021/es5030977

Sebire, M., Scott, A.P., Tyler, C.R., Cresswell, J., Hodgson, D.J., Morris, S., Sanders, M.B., Stebbing, P.D., Katsiadaki, I., 2009. The organophosphorous pesticide, fenitrothion, acts as an anti-androgen and alters reproductive behavior of the male three-spined stickleback, Gasterosteus aculeatus. Ecotoxicology 18, 122–133. https://doi.org/10.1007/s10646-008-0265-2

Serçinoğlu, O., Bereketoglu, C., Olsson, P.E., Pradhan, A., 2021. In silico and in vitro assessment of androgen receptor antagonists. Comput. Biol. Chem. 92. https://doi.org/10.1016/j.compbiolchem.2021.107490

Siriki, K., Yao, K.M., Gnonsoro, U.P., Trokourey, A., 2021. Transboundary river water pesticide pollution in historical agriculture areas in West Africa: a case study in the Comoe, Bia, and Tanoe rivers (Cote d'Ivoire). Arab. J. Geosci. 14. https://doi.org/10.1007/s12517-021-08294-7

Spirhanzlova, P., De Groef, B., Nicholson, F.E., Grommen, S.V.H., Marras, G., Sébillot, A., Demeneix, B.A., Pallud-Mothré, S., Lemkine, G.F., Tindall, A.J., Du Pasquier, D., 2017. Using short-term bioassays to evaluate the endocrine disrupting capacity of the pesticides linuron and fenoxycarb. Comp. Biochem. Physiol. Part - C Toxicol. Pharmacol. 200, 52–58. https://doi.org/10.1016/j.cbpc.2017.06.006

Sun, H., Xu, L.-C., Chen, J.-F., Song, L., Wang, X.-R., 2006. Effect of bisphenol A, tetrachlorobisphenol A and pentachlorophenol on the transcriptional activities of androgen receptor-mediated reporter gene. Food Chem. Toxicol. 44, 1916–1921. https://doi.org/10.1016/j.fct.2006.06.013

Swan, S.H., Elkin, E.P., Fenster, L., 2000. The question of declining sperm density revisited: An analysis of 101 studies published 1934-1996. Environ. Health Perspect. 108, 961–966. https://doi.org/10.1289/ehp.00108961

Tan, M.E., Li, J., Xu, H.E., Melcher, K., Yong, E.L., 2015. Androgen receptor: Structure, role in prostate cancer and drug discovery. Acta Pharmacol. Sin. 36, 3–23. https://doi.org/10.1038/aps.2014.18

Terouanne, B., Nirdé, P., Rabenoelina, F., Bourguet, W., Sultan, C., Auzou, G., 2003. Mutation of the androgen receptor at amino acid 708 (Gly→Ala) abolishes partial agonist activity of steroidal antiandrogens. Mol. Pharmacol. 63, 791–798. https://doi.org/10.1124/mol.63.4.791

van Leeuwen, S.P., Bovee, T.F., Awchi, M., Klijnstra, M.D., Hamers, A.R., Hoogenboom, R.L., Portier, L., Gerssen, A., 2019. BPA, BADGE and analogues: A new multi-analyte LC-ESI-MS/MS method for their determination and their in vitro (anti)estrogenic and (anti)androgenic properties. Chemosphere 221, 246–253. https://doi.org/10.1016/j.chemosphere.2018.12.189

Vinggaard, A.M., Niemelä, J., Wedebye, E.B., Jensen, G.E., 2008. Screening of 397 chemicals and development of a quantitative structure-activity relationship model for androgen receptor antagonism. Chem. Res. Toxicol. 21, 813–823. https://doi.org/10.1021/tx7002382

Wang, C., Niu, R., Zhu, Y., Han, H., Luo, G., Zhou, B., Wang, J., 2014. Changes in memory and synaptic plasticity induced in male rats after maternal exposure to bisphenol A. Toxicology 322, 51–60. https://doi.org/10.1016/j.tox.2014.05.001

Wang, H., Ding, Z., Shi, Q.-M., Ge, X., Wang, H.-X., Li, M.-X., Chen, G., Wang, Q., Ju, Q., Zhang, J.-P., Zhang, M.-R., Xu, L.-C., 2017. Anti-androgenic mechanisms of Bisphenol A involve androgen receptor signaling pathway. Toxicology 387, 10–16. https://doi.org/10.1016/j.tox.2017.06.007

Wang, Q., Yang, H., Yang, M., Yu, Y., Yan, M., Zhou, L., Liu, X., Xiao, S., Yang, Y., Wang, Y., Zheng, L., Zhao, H., Li, Y., 2019. Toxic effects of bisphenol A on goldfish gonad development and the possible pathway of BPA disturbance in female and male fish reproduction. Chemosphere 221, 235–245. https://doi.org/10.1016/j.chemosphere.2019.01.033

Wang, S., Liu, S., Liu, H., Wang, J., Zhou, S., Jiang, R.J., Bendena, W.G., Li, S., 2010. 20-Hydroxyecdysone reduces insect food consumption resulting in fat body lipolysis during molting and pupation. J. Mol. Cell Biol. 2, 128–138. https://doi.org/10.1093/jmcb/mjq006

Waters, K.M., Safe, S., Gaido, K.W., 2001. Differential gene expression in response to methoxychlor and estradiol through ERα, ERβ, and AR in reproductive tissues of female mice. Toxicol. Sci. 63, 47–56. https://doi.org/10.1093/toxsci/63.1.47

Wei, Y., Han, C., Li, S., Cui, Y., Bao, Y., Shi, W., 2020. Maternal exposure to bisphenol A during pregnancy interferes ovaries development of F1 female mice. Theriogenology 142, 138–148. https://doi.org/10.1016/j.theriogenology.2019.09.045

Wickham, H., Averick, M., Bryan, J., Chang, W., McGowan, L.D., Francois, R., Grolemund, G., Hayes, A., Henry, L., Hester, J., Kuhn, M., Pedersen, T.L., Miller, E., Bache, S.M., Muller, K., Ooms, J., Robinson, D., Seidel, D.P., Spinu, V., Takahashi, K., Vaughan, D., Wilke, C., Woo, K., Yutani, H., 2019. Welcome to the {tidyverse}. J. Open Source Softw. 4, 1686. https://doi.org/10.21105/joss.01686

Willi, R.A., Castiglioni, S., Salgueiro-González, N., Furia, N., Mastroianni, S., Faltermann, S., Fent, K., 2020. Physiological and Transcriptional Effects of Mixtures of Environmental Estrogens, Androgens, Progestins, and Glucocorticoids in Zebrafish. Environ. Sci. Technol. 54, 1092–1101. https://doi.org/10.1021/acs.est.9b05834

Xu, L.-C., Sun, H., Chen, J.-F., Bian, Q., Qian, J., Song, L., Wang, X.-R., 2005. Evaluation of androgen receptor transcriptional activities of bisphenol A, octylphenol and nonylphenol in vitro. Toxicology 216, 197–203. https://doi.org/10.1016/j.tox.2005.08.006

Xu, L.C., Sun, H., Chen, J.F., Bian, Q., Song, L., Wang, X.R., 2006. Androgen receptor activities of p,p′-DDE, fenvalerate and phoxim detected by androgen receptor reporter gene assay. Toxicol. Lett. 160, 151–157. https://doi.org/10.1016/j.toxlet.2005.06.016

Xu, X. hong, Zhang, J., Wang, Y. min, Ye, Y. ping, Luo, Q. qing, 2010. Perinatal exposure to bisphenol-A impairs learning-memory by concomitant down-regulation of N-methyl-d-aspartate receptors of hippocampus in male offspring mice. Horm. Behav. 58, 326–333. https://doi.org/10.1016/j.yhbeh.2010.02.012

Yamaguchi, A., Ishibashi, H., Arizono, K., Tominaga, N., 2015. In vivo and in silico analyses of estrogenic potential of bisphenol analogs in medaka (Oryzias latipes) and common carp (Cyprinus carpio). Ecotoxicol. Environ. Saf. 120, 198–205. https://doi.org/10.1016/j.ecoenv.2015.06.014

Yamazaki, E., Yamashita, N., Taniyasu, S., Lam, J., Lam, P.K.S., Moon, H.B., Jeong, Y., Kannan, P., Achyuthan, H., Munuswamy, N., Kannan, K., 2015. Bisphenol A and other bisphenol analogues including BPS and BPF in surface water samples from Japan, China, Korea and India. Ecotoxicol. Environ. Saf. 122, 565–572. https://doi.org/10.1016/j.ecoenv.2015.09.029

Yan, Z., Liu, A., Yan, K., Wu, H., Han, Z., Guo, R., Chen, M., Yang, Q., Zhang, S., Chen, J., 2017. Yan et al. 2017_Bisphenol analogues in surface water and sediment from the shallow Chinese freshwater lakes.pdf 318–328.

Yang, L., Zha, J., Zhang, X., Li, W., Li, Z., Wang, Z., 2010. Alterations in mRNA expression of steroid receptors and heat shock proteins in the liver of rare minnow (Grobiocypris rarus)

exposed to atrazine and p,p'-DDE. Aquat. Toxicol. 98, 381–387. https://doi.org/10.1016/j.aquatox.2010.03.010

Zhang, H., Zhang, Y., Li, J., Yang, M., 2019. Occurrence and exposure assessment of bisphenol analogues in source water and drinking water in China. Sci. Total Environ. 655, 607–613. https://doi.org/10.1016/j.scitotenv.2018.11.053

Zhang, Jianyun, Zhang, Jing, Liu, R., Gan, J., Liu, J., Liu, W., 2016. Endocrine-Disrupting Effects of Pesticides through Interference with Human Glucocorticoid Receptor. Environ. Sci. Technol. 50, 435–443. https://doi.org/10.1021/acs.est.5b03731

Acknowledgment

I would like to express my sincere gratitude to all the individuals who have contributed to the completion of my research. Their invaluable support and assistance have made this endeavor possible.

First and foremost, I deeply thank Professor Akira Kubota, my research supervisor, for his patient guidance, enthusiastic encouragement, and valuable critiques throughout my work. I am truly grateful for his acceptance into the toxicology laboratory and his continuous support in various aspects, including research, academic conferences, and more. I extend my best wishes to him for continued success and growth as an influential leader in the field of research.

I would also like to acknowledge and thank my co-supervisors, Assistant Professor Akihiro Kamikawa and Yoshikage Muroi, whose advice and suggestions have played a pivotal role at every stage of my research.

Furthermore, I am filled with gratitude towards Assistant Professor Yusuke Kawai for his prompt inspirations and insightful responses to my questions, which have significantly contributed to my personal and professional development.

Special appreciation goes to Professor Hiroshi Ishibashi (Ehime University) and Professor Masashi Hirano (Tokai University) for their invaluable *in silico* support in this study.

I am also grateful for the technical support received from Yao Butsuda and Hazuki Kida from Obihiro University of Agriculture and Veterinary Medicine.

I extend my deepest appreciation to Associate Professor Daisuke Kondoh for his guidance in laboratory techniques that will undoubtedly benefit my future career.

I am immensely grateful to my friends and colleagues for their companionship and for providing enjoyable moments. Their insightful comments and constructive suggestions have significantly contributed to the development of my research work.

I would like to express my sincere thanks to Obihiro University of Agriculture and Veterinary Medicine for providing the necessary resources and a supportive environment throughout my research journey in Japan. Their kind hospitality is greatly appreciated.

I am privileged to express my gratitude to the JAPAN SOCIETY FOR THE PROMOTION OF SCIENCE for their financial support, which has allowed me to fully focus on my studies in Japan. I am proud to have been selected as a scholar by this esteemed foundation that empowers young researchers to pursue their dreams and achieve their goals.

I would like to extend my deepest appreciation to my father An-nai Yang, mother Ming-e Liu, and husband Che-Hsuan Huang, for their unwavering encouragement and dedicated support in both my research and personal life. Your continuous support and belief in me have been a constant source of strength throughout this journey.

To all those mentioned above, as well as to everyone else who has supported me along the way, this research is dedicated to you. From the bottom of my heart, thank you all for your invaluable contributions.